

Classification du neuroblastome

A. The International Neuroblastoma Staging System (INSS)

B. The INRG Staging System

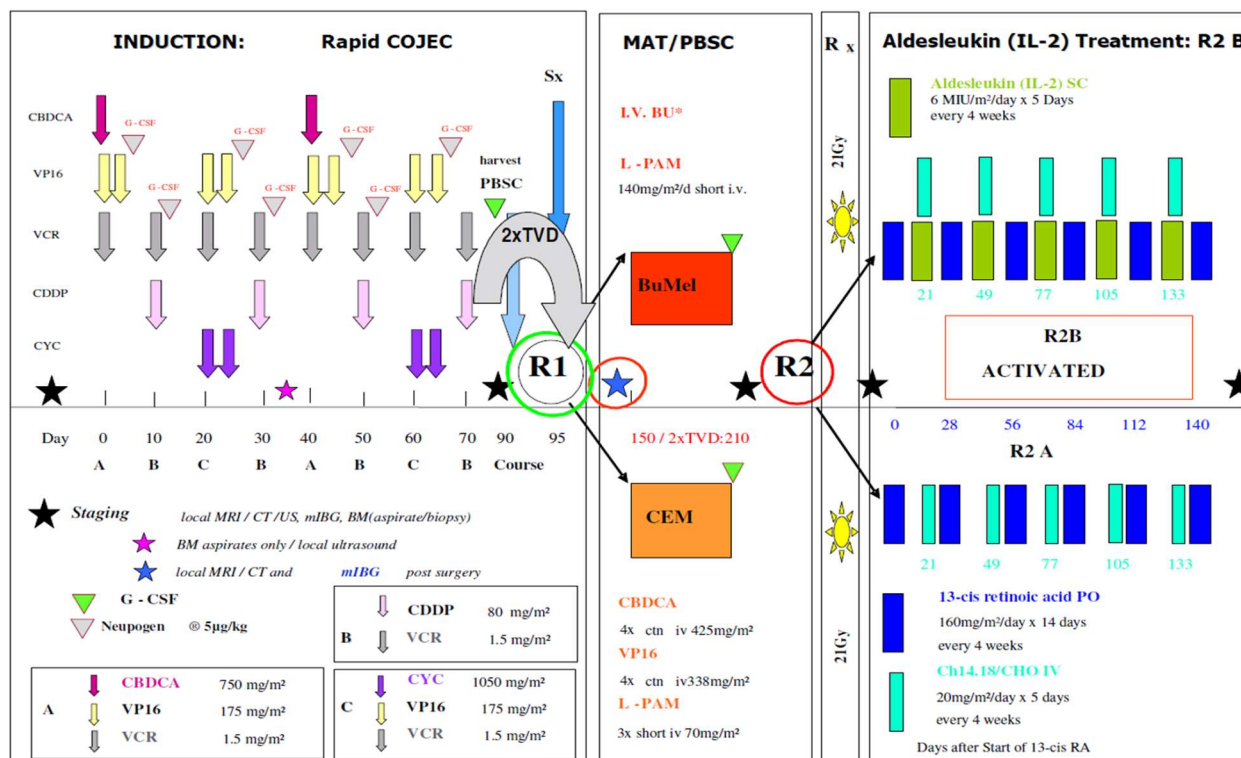
A

Table 4. The International Neuroblastoma Staging System (INSS) [34, 35]	
Stage 1:	Localized tumor* with complete gross excision, with or without microscopic residual disease; representative ipsilateral lymph nodes negative for tumor microscopically (nodes attached to and removed with the primary tumor may be positive).
Stage 2A:	Localized tumor with incomplete gross excision; representative ipsilateral nonadherent lymph nodes negative for tumor microscopically.
Stage 2B:	Localized tumor with or without complete gross excision, with ipsilateral nonadherent lymph nodes positive for tumor. Enlarged contralateral lymph nodes must be negative microscopically.
Stage 3:	Unresectable tumor infiltrating across the midline** with or without regional lymph node involvement; or localized unilateral tumor with contralateral regional lymph node involvement; or midline tumor with bilateral extension by infiltration (unresectable) or by lymph node involvement.
Stage 4:	Any primary tumor with dissemination to distant lymph nodes, bone, bone marrow, liver, skin and/or other organs (except as defined in Stage 4S).
Stage 4S:	Localized primary tumor (as defined for Stage 1, 2A, or 2B), with dissemination limited to skin, liver, and/or bone marrow*** (limited to infants less than one year of age).
* Multifocal primary tumors (e.g., bilateral adrenal primary tumors) should be staged according to the greatest extent of disease, as defined above, and followed by a subscript "M" (e.g., 3 _M).	
** The midline is defined as the vertebral column. Tumors originating on one side and "crossing the midline" must infiltrate to or beyond the opposite side of the vertebral column.	
*** Marrow involvement in stage 4S should be minimal, i.e., less than 10% of total nucleated cells identified as malignant on bone marrow biopsy or on marrow aspirate. More extensive marrow involvement would be considered to be stage 4. The mIBG scan (if done) should be negative in the marrow.	

B

INRG Stage	Age (months)	Histologic Category	Grade of Tumor Differentiation	MYCN	11q Aberration	Ploidy	Pretreatment Risk Group
L1/L2		GN maturing; GNB intermixed					A Very low
L1		Any, except GN maturing or GNB intermixed		NA			B Very low
				Amp			K High
L2	< 18	Any, except GN maturing or GNB intermixed		NA	No		D Low
					Yes		G Intermediate
	≥ 18	GNB nodular; neuroblastoma	Differentiating	NA	No		E Low
			Poorly differentiated or undifferentiated	NA	Yes		H Intermediate
				Amp			N High
M	< 18			NA		Hyperdiploid	F Low
	< 12			NA		Diploid	I Intermediate
	12 to < 18			NA		Diploid	J Intermediate
	< 18			Amp			O High
	≥ 18						P High
MS					No		C Very low
	< 18			NA	Yes		Q High
				Amp			R High

Annexe 2 : Protocole HRNBL1



* Dosage given according to body weight. For details of Busilvex® see Appendix “Drug Information”, 23.9.

R1

ENLARGED ELIGIBILITY CRITERIA ALLOWING **2TVD** CHEMOTHERAPY CYCLES IN ADDITION, IF INSUFFICIENT RESPONSE TO RAPID COJEC TO REACH PREVIOUS R1 RESPONSE CRITERIA

INFANTS : SPECIAL GUIDELINES AND DRUG DOSING IN THE RELEVANT CHAPTERS OF AMENDED PROTOCOL!

TVD: Topotecan 1.5mg/m²/day for 5 days short infusion, Doxorubicin 22.5mg/m² /24 ctn infusion, Vincristine 1mg/m²/day 48h ctn infusion. SPECIAL GUIDELINES AND DRUG DOSING IN THE RELEVANT CHAPTERS OF AMENDED PROTOCOL!

R2

ENLARGED ELIGIBILITY CRITERIA ALLOWING ALL PATIENTS REGISTERED ON HR-NBL-1/SIOPEN AND HAVING RECEIVED MAT/PBSC TO RECEIVE CH14.18/CHO WITH OR WITHOUT ALDESLEUKIN (IL-2) IF R2 RANDOMISED

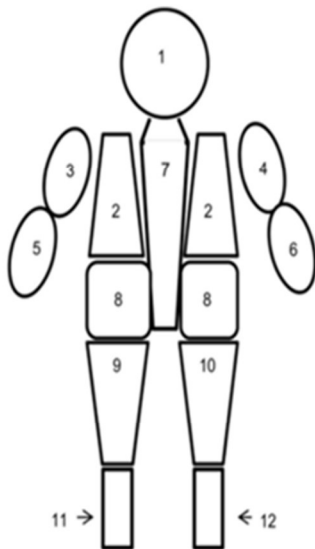
Note:

Once results of R1 become available the superior arm of the randomisation or in case of equivalent results the current standard arm (BUMEL) will be continued until R2 may be closed.

Annexe 3 : Cohorte de patients

		primitive						volu								
Age	Sex	mass	Metastases / Local extension	LDH	MYCN	SIOPEN	MIBG	me	surgery	Response	INRC	DC	OS	Progression	PFS	
1	45	girl	surrenal	marrow, pulmonary and pleural	1183	0	51	0	1143	0	1	RP	1	14	1	8
2	50	boy	surrenal	nods, marrow, renal and serous	3300	1	45	0	825	1	1	RP	1	15	1	15
3	54	boy	surrenal	bones, marrow and mediastinal	712	1	34	0	434	1	1	RP	1	20	1	13
4	54	girl	surrenal	nods, bones and marrow	1790	1	39	0	273	1	1	RC	0	118	1	59
5	11	boy	surrenal	nods, bones, marrow, mediastinal, renal, pulmonary, medullar canal,	3544	1	0	1		1	1	RP	0	107	1	9
6	50	boy	thoracic	nods, bones, marrow, medullar canal, serous	302	0	33	0	157	0	1	RC	1	42	1	27
7	16	boy	surrenal	nods, bones, marrow, mediastinal, renal, serous	2520	1	0	1		0	1	RP	1	5	1	5
8	24	boy	surrenal	bones and marrow	830	0	30	0	10	1	1	RC	0	96	0	96
9	27	boy	dominal	nods, bones, marrow and renal	842	1	2	0	508	1	1	RC	0	104	0	104
10	45	boy	surrenal	nods, bones and marrow	1370	0	27	0	0,5	1	1	RP	0	97	0	97
11	47	boy	surrenal	bones and marrow	508	0	40	0	40	1	1	RC	1	67	1	44
12	13	boy	surrenal	no one	879	1	0	0	189	1	1	RC	1	10	1	9
13	28	boy	cervicothoracic	marrow, medullar canal	882	0	0	0	142	1	1	RC	0	96	0	96
14	21	boy	abdominal	renal	1689	1	1	0	905	1	1	RC	0	96	0	96
15	30	girl	abdominal	nods, bones, renal and serous	2126	1	2	0	258	0	1	RP	1	6	1	4
16	44	girl	surrenal	marrow	1163	0	60	0	385	1	1	RP	1	43	1	31
17	31	boy	surrenal	bones	707	0	38	0	411	1	1	RP	1	54	1	38
18	48	boy	abdominal	nods and marrow	1481	1	0	0	444	1	1	RC	1	53	1	44
19	27	boy	surrenal	bones and marrow	361	0	43	0	41	1	1	RP	0	75	1	8
20	27	girl	surrenal	nods, bones, marrow and hepatic	22022	1	47	0	408	0	0	SD	1	4	1	3
21	140	boy	surrenal	nods, bones and mediastinal	3230	1	53	0	227	1	1	RP	1	10	1	10
22	28	girl	abdominal	nods, marrow, mediastinal and medullar canal	464	0	14	0	75,6	1	1	RP	1	37	1	18
23	36	girl	olfactive	nods, bones and marrow	332	0	18	0		0	1	RC	1	26	1	13
24	33	girl	abdominal	nods, marrow and mediastinal	1041	0	40	0	6,9	1	1	RC	0	57	0	57
25	111	boy	surrenal	bones and marrow	317	0	10	0	441	0	1	RP	1	26	1	24
26	33	girl	abdominal	marrow and renal	1216	1	0	0	870	1	1	RP	1	11	1	11
27	74	girl	surrenal	marrow, mediastinal and renal	1437	1	38	0	1099	1	1	RC	0	48	0	48
28	34	girl	abdominal	nods, bones and marrow	712	0	15	0	20,3	1	1	RP	1	30	1	18
29	65	boy	abdominal	nods, bones, marrow, medullar canal and psoas	579	1	0	0	265	0	1	RC	0	49	0	49
30	101	boy	surrenal	nods, bones and marrow	637	1	12	0	61,3	1	1	RC	0	45	0	45
31	25	girl	abdominal	bones, marrow and mediastinal	434	0	29	0	36,4	1	1	RC	0	43	0	43
32	107	boy	surrenal	bones, marrow, medullar canal and hepatic	6628	1	38	0	23,4	1	1	RC	1	21	1	14
33	29	girl	abdominal	bones and marrow	372	0	36	0	132	0	1	RP	1	33	1	24
34	36	boy	surrenal	marrow, renal and pulmonary	2683	1	3	0	105	1	1	RP	1	10	1	9
35	44	boy	abdominal	nods, bones, marrow and mediastinal	316	0	27	0	429	1	1	RC	0	35	0	35
36	26	girl	surrenal	no one	666	0	0	0	187	1	1	RC	0	35	0	35
37	54	boy	surrenal	nods and marrow	2572	1	1	0	46	1	1	RP	1	33	1	29
38	16	girl	abdominal	medullar canal	456	0	0	0	212	1	1	RC	1	26	1	17
39	11	boy	surrenal	nods, marrow and renal	3790	1	0	0	646	1	1	RC	0	29	0	29
40	53	girl	abdominal	bones, marrow and hepatic	773	0	39	0	903	1	1	RC	1	17	1	21
41	22	girl	surrenal	nods and bones	416	0	0	1		1	1	RC	0	31	1	1
42	17	girl	abdominal	bones, marrow, mediastinal, medullar canal, serous and hepatic	356	0	10	0	70,4	1	1	RP	0	28	0	28
43	26	girl	surrenal	nods, bones, renal and serous	3097	1	0	0	926	1	1	RC	0	25	0	25
44	110	boy	thoracique	bones, marrow and medullar canal	618	0	45	0	57	0	1	RP	0	24	0	24
45	47	boy	surrenal	bones and marrow	626	0	32	0	141	1	1	RP	0	22	0	22
46	39	girl	abdominal	nods and marrow	604	0	40	0	84	0	0	SD	0	13	0	13
47	37	boy	surrenal	pancréatique	2328	1	1	0	432	1	1	RP	0	12	0	12
48	21	girl	abdominal	bones, marrow and mediastinal	5198	1	59	0	555	0	1	RP	1	5	1	5
49	38	boy	abdominal	no one	423	0	2	0	410	1	1	RP	0	10	0	10

Annexe 4 : Score SIOPEP



Before performing scintigraphy, we must avoid interfering treatment and protect thyroid with stable iodine thyroid saturation.

Then, in practice, I123 mIBG is slowly injected by peripheral venous pathway (to avoid side effect), and the radiation gamma Recording (346keV) come after 24h, with an exposition Time to radiation <10minutes if patient cooperate.

To score patient, we divide the skeleton in 12 segments, and for each of whom, extension of lesions is noted as :

- 0 : no lesion
- 1 for 1 lesion
- 2 for 2 lesions
- 3 for 3 lesions
- 4 for > 3 lesions but <50% of the concerned segment
- 5 for diffuse disease but <95% of hole segment
- 6 for diffuse disease > 95% of hole segment

Annexe 5 : Temps de doublement cellulaire

Accession/Cell line name	Origin	Sex	Age	Risk Staging	Métastasis	Nmyc	In vivo/vitro	CDT (h)
CVCL9880/VA N BR	H	M	72	STADE II	ABDOMINAL	NC	NC	36
CVCL 6594/CHLA15	H	F	18	NC	MO	NC	NC	21
CVCL 9898/SK N BE(1)	H	M	22	NC	MO	NC	NC	96
CVCL E058/MC NB 1	H	M	24	NC	MO	NC	NC	35
CVCL 7135/SMS MSN	H	M	60	NC	MO	NC	NC	85
CVCLS102/JH	H	M	11	ABDO STADE III	NC	NC	NC	35,7
CVCL B322/KELLY	H	F	12	ALK	NC	NC	NC	35
CVCL AQ17/CHLA 61	H	M	14	NC	NC	NC	NC	102
CVCL 9896/NUB 6	H	NC	21	NC	NC	NC	NC	48
CVLC S099/AS	H	F	33	NC	NC	NC	NC	35,8
CVCL S100/AST	H	M	36	NC	NC	NC	NC	40,7
CVCL IV95/CH9100S	H	F	144	NC	NC	NC	IN VITRO	26
CVCL AQ24/COG N 421	H	M	NC	NC	NC	NC	NC	65
CVLC AQ16/CHLA 53	H	NC	NC	P53	NC	NC	NC	92
CVCL 3041/NB(TU)1	H	F	20	STADE III	NC	NC	NC	49
CVCL IV94/CHP100L	H	F	144	TP53	NC	NC	IN VITRO	21
CVCL 0019/SH SY5Y SKNAS	H	F	48	IV N TYPE	MO	NEG	NC	50
CVCL 2136/NBL S	H	M	43	NC	MO	NEG	NC	37
SKNAS	H				MO	NEG		37
CVCL 2136/NBL S	H	M	43	NC	NC	NEG	NC	36
CVCL AQ11/CHLA 12	H	NC	NC	P53	NC	NEG	NC	65
CVCL 0346/IMR 32	H	M	13	METASTATIC	ABDOMINAL	NMYC	IN VITRO	48
CVCL 9896/NUB 7	H	M	6	INTERMEDIATE(1)	ADRENAL	NMYC	NC	38
CVCL 1234/GOTO	H	M	13	NC	ADRENAL	NMYC	NC	48
CVCL 1771/TGW	H	M	23	NC	ADRENAL	NMYC	IN VIVO	32
CVCL 1695/SiMa	H	M	20	NC	ADRENAL	NMYC	NC	74
CVCL 2141/NGP	H	M	30	IV	LUNG	NMYC	NC	60
CVCL 144/NB1	H	M	27	NC	LYMPH NODE	NMYC	NC	45
CVCL 0167/SK N BE(2) M17	H	M	22	IV N TYPE / TP53	MO	NMYC	NC	24
CVCL 2143/NMB	H	F	10	IV NC	MO	NMYC	NC	45
CVCL W474/JK NB1	H	M	12	NC	MO	NMYC	NC	48
CVCL 8904/PER 106	H	M	17	NC	MO	NMYC	IN VITRO	252
CVCL 2548/LA1 55n	H	M	24	NC	MO	NMYC	NC	48
CVCL 7136/SMS SAN	H	F	36	NC	MO	NMYC	NC	71
CVCL 9902/UKF NB 2	H	NC	NC	STADE IV	MO	NMYC	NC	22,5
CVCL 9907/UKF NB 4	H	NC	NC	STADE IV	MO	NMYC	NC	20
CVCL 9904/UKF NB 3	H	NC	NC	STADE IV +	MO	NMYC	NC	22
CVCL 2105/LS	H	F	16	ABDO - STADE III	NC	NMYC	NC	45
CVCL AQ23/COG N 415	H	NC	24	ALK	NC	NMYC	IN VITRO	50
CVCL 5627/NB 1643	H	M	36	ALK - ADRENAL	NC	NMYC	NC	43
CVCL 7133/SMS KCN	H	M	11	ALK - EBV	NC	NMYC	NC	109
CVCL 7131/SMS KAN	H	F	36	N TYPE	NC	NMYC	NC	95
CVCL 1124/CHP134	H	M	13	NC	NC	NMYC	IN VITRO	57,6
CVCL 1123/CHP126	H	F	14	NC	NC	NMYC	IN VITRO	44,5
CVCL AQ25/COG N 440	H	NC	18	NC	NC	NMYC	NC	65
CVCL 1829/LA N 2	H	F	36	STADE II	NC	NMYC	NC	60
CVCL AQ22/COG N 399	H	M	NC	NC	NC	NEG	NC	40
CVCL AQ21/COG N 347	H	M	24	P53	NC	NEG	NC	126
CVCL AQ18/COG N 291	H	NC	NC	P53	NC	NEG	NC	224
IGR N91								66
NB39								48
NB45								240
CHP212								20
HTB10								54
HSNB								50
P.YEUNG 20								50,88
P. YEUNG 50								74,16
P. YEUNG 80								88,56

H: Human, F: Female, M: Male, NEG: Negative, NC: Unknown

Abbreviations

Anti GD2 : anticorps anti GD2 (Dinutuximab)

AP-HM : Assistance Publique Hôpitaux de Marseille

CDT : Temps de doublement cellulaire

DPI : Dossier Patient informatisé

Scanner CTAP: Scanner Cervico-Thoraco-Abdomino-Pelvien

EFS : Event Free Survival.

HR : Hazard Ratio

HRNB : High-Risk Neuroblastoma

IC : Intervalle de confiance 95%

IL-2: Interleukine 2

INRC : International Neuroblastoma Response Criteria

INGR : International Neuroblastoma Risk Group

IRM : Imagerie par Résonance Magnétique

KM : Kaplan Meier

LDH : Lactate Deshydrogenase

OS : Overall Survival

MIBG : meta-Iodine-Benzyl-Guanidine

PFS : Progression Free Survival

PCR : Polymerase Chain Reaction

SIOPEN : International Society of Pediatric Oncology Europe Neuroblastoma Group

UHRNB : Ultra-High-Risk Neuroblastoma

Contents

I. Introduction.....	6
II. Material and methods.....	7
A- Cohort collection and data.....	7
B- Mathematical model.....	9
C- Statistical analysis	12
D- Authorizations and Ethic	12
III. Results: Description of the cohort.....	12
A- Patients and Tumor Characteristics (Figure 2).....	12
B- Patient outcomes	13
C- Mathematical Modeling	13
IV. Results: Classical Prognosis Factor Analyses.....	14
A- PFS analyses (Figure 5).....	14
B- OS analyses (Figure 5)	14
V. Results: Mechanistic Model.....	15
A- Establishment of the Mathematical Model.....	15
B- Validation of the model.....	15
C- Survival analyses and Prognosis Value of the Model (Figure 6).....	15
VI. Determination of an Ultra High-Risk Neuroblastoma?	16
VII. Discussion	16
VIII. Conclusion.....	19
IX. References.....	19
X. Figures :	24
Figure 1: Clinical and Preclinical History of neuroblastoma: simulation of growth and dissemination of neuroblastoma by mechanistic mathematical modeling	24
Table 1: Cells line characteristics for establishment of cell doubling time (CDT)	25

Figure 2: Patients and Tumor Characteristics.....	26
Figure 3: Validation of the model:	27
Figure 4: OS and PFS for overall population	28
Figure 5: PFS and OS - Classical statistical analysis	29
Figure 6: Survival analyses and Prognosis Value of mechanistic model.....	30
Figure 7: Survival analysis and Research of factors associated with PFS > 18months	31
XI. <i>Appendix</i>	32
Appendix 1 : Neuroblastoma classification.....	32
Appendix 2 : HRNBL Protocol	33
Appendix 3 : Patient Cohort	34
Appendix 4 : SIOPEN Scoring.....	35
Appendix 5 : Cells Doubling Time (36).....	36

Descriptive and prognostic value of a computational metastases model in high-risk neuroblastoma

**Coline Sentis¹, Sébastien Benzekry², Laëtitia Tessonnier^{3,4}, Carole Coze^{1,3}, Nicolas
André^{1,3,5},**

1 : Paediatric Hematology and Oncology Department, Hôpital pour enfant de La Timone, AP-HM, Marseille, France,

2 : MONC Team, INRIA, Bordeaux Sud-Ouest and Institut de Mathématiques de Bordeaux, France.

3 : Aix Marseille University

4 : Department of Nuclear Medicine, Hôpital de La Timone, AP-HM, Marseille, France

5 : SMARTc unit, Centre de Recherche en Cancérologie de Marseille Inserm U1068 Aix Marseille Univ, Marseille France

Abstract

BACKGROUND: High Risk Neuroblastoma (HRNB), is the second most frequent solid tumor in children. Its prognosis remains poor even with multimodal therapies and risk-adapted strategies (5years Event Free Survival (EFS) <50%). Several mathematical models were developed over recent years to describe primary and metastatic tumor burden, but none in neuroblastoma and their prognosis value has yet to be determined.

AIMs to build a mechanistic model, check its validity, and assess its prognostic value.

MATERIAL AND METHODS: We established a mechanistic mathematical model for HRNB, using the tumor size associated with 2 coefficients: μ (dissemination) and α (growth). The model was calibrated using the lactate dehydrogenase (LDH) circulating level and the MIBG SIOPEN score. Data from a cohort of 49 HRNB patients treated according to the HRNBL1 recommendations over the last 10 years were used.

RESULTS The model was able to describe the metastatic burden of the disease. We found existence of a subgroup of HRNB with poorer prognosis in PFS and OS for a high LDH level (70-80th) and SIOPEN score at diagnosis (90th percentile) with a $p < 0,05$ with classical survival analysis, confirmed in our model for the LDH rate. We found also that a high μ value is associated with a better OS ($p < 0,05$)

CONCLUSION: Mathematical mechanistic model can describe and predict tumoral burden using clinico-biologic data in human patients. It allowed the identification of a new μ risk factors, associated with better outcomes in OS in our population. The physiological substrate underlying these results have yet to be explored.

I. Introduction

Neuroblastoma is the second solid tumor in children (8-10% children cancers in USA and Europe) with a median age at diagnosis of 2 years (1), (2). Neuroblastoma is responsible of almost 15% of childhood deaths by cancer (3). Neuroblastoma is a quite heterogeneous disease at clinical, histological and biological levels (4). Consequently, its prognostic spectrum is also wide (5). The International Neuroblastoma Risk Group (INRG) proposed in 2009 a classification model depending of cancer data (dissemination of neuroblastoma, histology category, grade of tumor differentiation, genetic abnormalities such as MYCN amplification (6) and patient age (3) (7) with a cut off of 18months (8) (Appendix 1). Therefore, neuroblastoma is currently divided in 3 groups: Low, Intermediate and High-Risk Neuroblastoma (HRNB), who display quite different survival rates. For patients treated according to the International Society for Paediatric Oncology European (SIOPEN) recommendations, the 5 years overall survival is more than 90% for the first group thanks to minimal therapeutics (surgery and/or chemotherapy or simple overseeing), 60 to 80% for the second (5) (according LINES recommendations) and < 50% for the last group whom representing nearly 50% of patients (according HRLBN1 recommendations) (3) ,(9), (10), (11), (12) despite intensive multimodal treatments. Furthermore, patients progressing during induction or after initial response to induction have a dismal 5years EFS (<20%) (13), (14). For these refractory patients, the current therapeutics are unsatisfactory, and new treatments are needed to try to reach better outcomes.

In the early sixties (15) efforts have been made to develop mathematical models to assist cancer research. Their aim was to understand tumor growth kinetics and metastatic dissemination (16) and to propose rational tools for the design of schedules of administration of chemotherapy (17,18).

Three main types of mathematical models can be distinguished. On one hand, highly complex, multiscale models try to integrate many biological data ranging molecular processes to cancer spreading at the whole organism level. This approach requires many parameters and consequently are often hard or impossible to reliably calibrate for clinical purpose (19). On the other hand, purely statistical model and artificial intelligence techniques rely on agnostic algorithms that try to learn directly patterns from the data (20). In between, mechanistic or semi-mechanistic models seek to describe only the main determinants of a cancer disease, for a given purpose (e.g., understanding

(21,22) or prediction (23,24) of metastatic relapse). To our knowledge no mechanistic model has been established and validated for neuroblastoma yet.

In this study, we have established a semi-mechanistic model of high-risk neuroblastoma (HRNB) to describe the metastatic burden using two coefficients: a patient specific parameter μ for the dissemination process and a patient nonspecific parameter α for the growth process. This model was built and validated with the clinical, biological and radiological data from a cohort of 49 with HRNB and treated according to the HRNBL1 protocol (10 and Appendix 2). We then evaluated the prognostic value of this model and tried to identify Ultra High-Risk patients.

Materials and Methods

Cohort collection and data

Our population is made up of 49 patients with HR-NB, treated according to HR-NBL1 protocol recommendations, treated in the pediatric hematology and oncology Unit of the children hospital of AP-HM between 26/11/2007 and 30/08/2018. (Appendix 3). We choose for entry date the study the date of diagnosis. For survival analyses, end date was either the date of patients' death or the date of the last news.

Inclusion Criteria are inclusion criteria of the HRNBL1 Protocol (10).

HRNBL1 Protocol: Details of the protocol are given in appendix 2. Briefly, induction chemotherapy with « rapid COJEC » or “modified N7 induction” was given for 10 weeks, followed by surgery if it's possible, then myeloablative chemotherapy with hematopoietic peripheral stem cell transplantation. Treatment was completed with radiotherapy and maintenance therapy with immunotherapy (antigGD2 \pm IL2) and retinoic acid for 6 months.

Collected Data: All data were gathered from Personalized Computerized Folder (PFC) by Axigate platform used in our University Hospital of Marseille, including neuroblastoma risk factors as age at diagnosis, LDH values who could be correlated to the total tumoral volume or as a reflect of a quick tumoral renewal (6), (10), (25), (26) or MYCN amplification, researched by PCR from peripheral blood and/or from primary or metastatic tumoral tissue at diagnosis and allows patient ranking as MYCN + if MYCN amplification was present in one of both collections.

The SIOPEN score (Appendix 4)

The meta-iodo-benzyl-guanidine (mIBG) is known to bind to neuroblastoma cells using iodine 123 (I123) (27) and the mIBG scintigraphy is consequently used to evaluate the extent of the neuroblastoma, in agreement with INRG. Indeed, almost 90% of neuroblastoma fix mIBG (28) both in primary tumor, and metastatic sites such as bones, bone marrow (29) or even soft tissues with a high sensibility (85-94%) (30). We used a semi quantitative score SIOPEN that was elaborated to predict extension and severity of the disease (31). A high score has been shown as pejorative but no reproducible cut off has not yet been found (28,31). We established the SIOPEN score with the data of PCF by Centricity program or by retrospective double scoring scintigraphy with an experiment nuclear doctor (*Dr Tessonnier*).

Tumor characteristics:

- *Location and size of primary tumor* was evaluated using radiological reports performed at diagnosis. Primary tumoral volumes were estimated by the formula: $\frac{4}{3} \pi abc$ with *a* as half longest axis, *b* as half medium axis and *c* as half little axis of an ellipsoid tumor.

- *Location of metastases and “total metastatic mass”*: We must search metastatic locations by Imaging, mIBG scintigraphy being currently the gold standard. But CTAP scan or MRI are also performed to confirm or detect possible visceral metastasis, difficult to highlight with scintigraphy and unrecorded by SIOPEN score. Metastasis location were mainly evaluated with MIBG. In addition, bone marrow location was also valuated with myelograms and bone marrow biopsies. Data were available on PFC.

Disease evolution data:

- *Date of the Best Treatment Response according the International Neuro-blastoma Response Criteria (INRC) criteria* (32): Complete Response or no visualizable disease, Partial Response or regression at least of 30% of the disease, Stable Disease or regression of <30% of the disease.

- *Date of Relapse or Disease Progression after regression under treatment* : Date on which an unfavorable evolution of disease has been highlighted by radiology (scanner and/or MRI), Nuclear imaging (TEP TDM and/or mIBG I123 scintigraphy MIBG). We defined Ultra-High-Risk (UHRNB) group as a group of patients who relapse or progress precociously, as soon as 18 months after diagnosis.

B. Mathematical model

The mathematical model was adapted from a previously published mathematical framework for description of metastases (22,24,33). This construct allows to simulate a cancer disease, including growth of the primary tumor (PT), as well as birth and growth of secondary lesions (Figure 1). We assumed growth of both the primary and secondary tumors to follow an exponential law:

$$S_p(t) = S(t) = e^{\alpha t},$$

where $S_p(t)$ and $S(t)$ denote the sizes of a primary and a secondary tumor (expressed in number of cells), starting from one cell at time $t = 0$. The parameter α denotes the proliferation rate and was estimated from the doubling time determined as explained above, using the following formula:

$$\alpha = \frac{\ln 2}{CDT}.$$

Assuming a birth rate of metastasis proportional to the size of the PT with parameter μ , the number of metastasis at time t is given by (22):

$$N(t) = \mu \int_0^t S_p(s) ds.$$

The parameter μ corresponds to the per day probability for each cell of the PT to spread and establish a distant metastasis. The total metastatic burden (total number of metastatic cells in the organism) is given by (24)

$$M(t) = \mu \int_0^t S_p(s) S(t-s) ds.$$

Visible metastases at time t (i.e. metastases with size larger than a visibility threshold S_{vis}) are the ones that were born early enough to have reached S_{vis} , that is, before $t - \tau_{vis}$, where τ_{vis} is the time to reach S_{vis} (see Figure 1). This time is given by $\tau_{vis} = \frac{\ln(S_{vis})}{\alpha}$ and the mass of only visible metastases can then be computed as:

$$M_{vis}(t) = \mu \int_0^{t-\tau_{vis}} S_p(s) S(t-s) ds = \mu \int_0^{t-\tau_{vis}} S_p(t-\tau_{vis}-s) S(s+\tau_{vis}) ds,$$

where τ_{vis} is the time to reach a visibility threshold S_{vis} starting from one cell. It is given by $\tau_{vis} = \frac{\ln(S_{vis})}{\alpha}$. The visibility threshold S_{vis} is considered as a model parameter. Numerical simulations of M and M_{vis} were performed using the fast Fourier transform algorithm as implemented in the *scipy* python package (python 3.7), exploiting the convolution structure of the equations (34)

For forward simulations of the model, a discrete version was employed with initiation time T_i and size S_i of the i -th metastasis given by:

$$T_i = \inf\{t > 0; N(t) \geq i\}, \quad S_i = e^{\alpha(t-T_i)}, \text{ for } t > T_i.$$

Calibration of the model: To determine the age of the tumor (or time of diagnosis T_d), we used the PT size and the assumption of exponential growth with rate α :

$$T_d = \frac{\ln(S_d)}{\alpha},$$

where S_d is the size of the PT at diagnosis. This quantity was derived from three diameters, obtained by Imaging measurements, which allowed computation of the PT volume assuming ellipsoidal shape. This volume was converted into a number of cells using the standard assumption of $1 \text{ mm}^3 \simeq 10^6$ cells (35)

Then, for each patient, two quantitative measurements were used to compare the metastatic model to the data: the SIOPEN score and the LDH blood level. The former was assumed to be a surrogate of the visible metastatic mass while the latter was assumed to represent the total cancer burden in the organism (PT + metastases), see Figure 1. Denoting with i superscript the quantities that depend on individual i and explicitly writing dependencies of the model functions on their parameters, we thus assumed:

$$\begin{aligned} SIOPEN^i &= M_{vis}(T_d^i; \mu^i, S_{vis}) \times (1 + \sigma \varepsilon^1), \quad \varepsilon^1 \sim \mathcal{N}(0,1) \\ LDH^i &= \left(\phi S_p(T_d^i) + M(T_d^i; \mu^i, S_{vis}) \right) \times (1 + \sigma \varepsilon^2), \quad \varepsilon^2 \sim \mathcal{N}(0,1) \end{aligned}$$

which expresses a proportional error model for the observations with standard deviation $\sigma = 0.1$, corresponding to a 10% measurement error. Note that only one parameter (μ^i) was patient specific. Maximization of the log-likelihood for the expression above leads to minimization of the following objective function:

$$l(S_{vis}, \phi, \mu^i) = l_{SIOPEN}(S_{vis}, \mu^i) + l_{LDH}(\phi, \mu^i)$$

$$\begin{aligned}
&= \frac{\left(SIOPEN^i - SIOPEN_{model}^i(S_{vis}, \mu^i)\right)^2}{2\left(\sigma SIOPEN_{model}^i(S_{vis}, \mu^i)\right)^2} \\
&\quad + \ln\left(\sigma\sqrt{2\pi}SIOPEN_{model}^i(S_{vis}, \mu^i)\right) + \frac{\left(LDH^i - LDH_{model}^i(\phi, \mu^i)\right)^2}{2\left(\sigma LDH_{model}^i(\phi, \mu^i)\right)^2} \\
&\quad + \ln\left(\sigma\sqrt{2\pi}LDH_{model}^i(\phi, \mu^i)\right)
\end{aligned}$$

with

$$\begin{aligned}
SIOPEN_{model}^i(\theta^i) &= M_{vis}(T_d^i; \mu^i, S_{vis}) \\
LDH_{model}^i(\theta^i) &= \phi S_p(T_d^i) + M(T_d^i; \mu^i, S_{vis}).
\end{aligned}$$

Minimization was performed by separating population-level and individual-level parameters, i.e.:

$$\begin{aligned}
\widehat{S_{vis}}, \widehat{\phi} &= \underset{S_{vis}, \phi}{\operatorname{argmin}} \sum_i \min_{\mu^i} l(S_{vis}, \phi, \mu^i) \\
\widehat{\mu}^i &= \underset{\mu^i}{\operatorname{argmin}} l(S_{vis}, \phi, \mu^i),
\end{aligned}$$

and was implemented using the Nelder-Mead algorithm of the *minimize* function of the *scipy* python package (python 3.7).

Cells doubling time (CDT) in neuroblastoma was an essential prerequisite of mathematical model establishment to estimate the growth potential of this cancer. Thus, we searched studies relating to CDT in PubMed and known CTD for specific neuroblastoma cell stains from a Cellosaurus (database of commercial cell population (36)). When they were available, age, sex, stage of neuroblastoma and/or the presence of metastasis and the NMyc status were referenced. All cells population were obtained from human patient, CDTs were established in vitro. (Appendix5) Of the 73 strains studied, 15 were excluded due to a lack of knowledge of the possible exposure to chemotherapy (all cells must be free of chemotherapy exposure to do not incite confusion).

In the end we had 57 cells populations. Average age of patients was 30.8months (median 22 months). In average, the CDT were of 62.4h (median 48h (20-258h)) (Table 1)

C. Statistical analysis

Due to ranges spanning several orders of magnitude, individual values of LDH levels and the mathematical parameter μ were log-transformed beforehand. Association between clinical variables and/or the individual mathematical parameter $\ln \mu$ with progression-free survival or overall survival was assessed using univariate and multivariate proportional hazard Cox regression models were used. The *lifelines* python package was used to fit the models. Resulting models were evaluated for their predictive power by computing the mean of Harrell's c-index (37) during a ten-folds cross-validation procedure.

D. Authorizations and Ethic

Authorization to perform the study was obtained at APHM (Public Assistance of Marseille's Hospitals) Health Data Access Portal (number request 32PTJ5)). We respect the Informatic and Liberty Law (1978) for the use of data.

III. Results: Description of the cohort

A. Patients and Tumor Characteristics (Figure 2)

- **Population:** 49 patients were included in our cohort. But 2 girls of 26 and 11 months have been included after diagnosis of low risk neuroblastoma and after their surgery treatment, due to an early progression. The MYCN status for both patients were negative but have changed for the younger one. We excluded 4 patients for the construction of the mathematical model as the date of inclusion in the HRNBL protocol was delayed when compared to the initial diagnosis.

- **Neuroblastoma known risk factors** (Figure 2A): In our cohort, median age was 36 months (11-140). LDH levels at diagnosis were high with a median level of 842 UI/L (302-22022) with laboratory standards that vary over time, but still < 300 UI/L. The SIOPEN score was overall high, with a median score of 27 (0-60). In our cohort, 3 patients who had a negative MIBG (no fixing primary tumor on scintigraphy) were excluded. Metastases were presents for most patients (87,6%). 45 patients (91.8%) had TDM, 11 patients MRI (22.4%). All patients benefited of bone marrow aspirate and or/biopsy (42 patients).

- Location and size of primary tumor

Location of primary tumor were adrenal for 55,1% patients (n=27) and abdominal for 34,7% (n=17). Details are given in Figure 2B. Primary tumoral median volume was 400cm³ (range 0.5cm³ -22265cm³).

- *Location of metastases* are detailed in figure 2C. The most frequent metastatic site was bone marrow (77,6% - n=38). Renal, medullar canal or pancreatic locations were considered as local extension of the disease.

B. Patient outcomes

All patients presented a response to overall chemotherapy. 23 patients had a complete response (46.9%), 24 a partial response (49%) and only 2 obtained just a lesion stability (4.1%). However only 20 patients did not progress (40,8% of patients). Among those who have progress (59,2%), 25 died (51% of all cohort patients). Details of patient's survival are showed in the Kaplan Meier (KM) curve (figure 4) The median for survival without progression was 29 months. At 3 years 44,1%, at 5years 29,1%. The median for overall survival (OS), time between the date of diagnosis and the date of last news, was 43 months. At 3years 55,8% and at 5years 38,9%.

C. Mathematical Modeling

To describe the metastatic state of HRNB patients, we developed a semi-mechanistic modeling approach whereby the metastatic process is reduced to two main phenomena: growth and dissemination (see Figure 1 and Methods). Growth was assumed to be exponential and the dissemination rate to be proportional to the primary tumor size, with a proportionality factor μ . This parameter is thus the per cell per day probability for a given cell in the primary mass to disseminate and form a metastatic colony at a distant site. To rely to the data and estimate μ^i in a patient i , we assumed that the LDH level was a surrogate of the total metastatic mass, whereas the SIOPEN score reflected the visible metastases only (see Figure 1 and Methods). We also used the primary tumor size at diagnosis to infer the age of the tumor and simulate the pre-diagnosis history of the disease. This analysis resulted in predicted ages of 75 ± 4 days (mean \pm standard deviation, media 76 days) between the first cancer cell and diagnosis. The model was able to accurately reproduce the LDH levels (Figure 3A). Descriptive power of the SIOPEN score was much less important (Figure 3B), with most patients either predicted to have no visible mass (SIOPEN = 0) despite visible mass in the data (SIOPEN >0), or conversely. The parameter

In μ revealed no correlation with either the log(LDH) ($R = 0.25$) or the SIOPEN ($R = 0.201$, Figure 3C), suggesting independent added value of this parameter – possibly informative of progression or survival – as compared to the data alone.

IV. Results: Classical Prognosis Factor Analyses

A-PFS analyses (Figure 5)

Using KM analysis, no differences by classical survival log rang test between patients were found for gender ($p=0,207$), MYCN status ($p=0,342$), age ($p=0,948$ with a cut off of 12 months and $p=0.255$ with a cutt off of 18 months). Nevertheless, a statistically significant difference in PFS was found for LDH rate (with a cut of off 1603UI/L (70th percentile)), $p=0,0385$. Similarly, a significant difference in PFS was found for SIOPEN score (with a cut off 45,4 (90th percentile), $p= 0.000861$).

With Cox regression model including individual features, confirmed by multivariate analyses, only LDH rate seems to present tendency for PFS with a Hazard Ratio (HR) of 1,6 (IC95%: 1-2,56), $p=0,05$ with a mean c-index in 10-fold cross-validation (MCI) of 0.618.

B- OS analyses (Figure 5)

Using KM analysis, no difference by the classical survival log rang test between patients were found for gender ($p=0,217$), MYCN status ($p=0,217$), or the age of patient whatever the cut-of ($p=0,217$ for cut off of 12 months, $p=0,706$ for one of 18months). A statistically significant difference in OS between patients was found for LDH levels with a cut-off of 2541UI/L (80th percentile), $p=0,0198$. There was also a statistically significant difference in OS between patients SIOPEN score with a cut-off of 45,4 (90th percentile), $p= 0.000169$.

With Cox regression model including individual features, confirmed by multivariate analyses, only LDH rate seems to present a difference statistically significant for OS with an HR of 1,74 (IC95%: 1,07-2,84), $p=0,0268$, with an MCI of 0.596

V. Results: Mechanistic Model

A. Establishment of the Mathematical Model

To describe the metastatic state of HRNB patients, we developed a semi-mechanistic modeling approach whereby the metastatic process is reduced to two main phenomena: growth and dissemination (see Figure 1 and Methods). Growth was assumed to be exponential and the dissemination rate to be proportional to the primary tumor size, with a proportionality factor μ . This parameter is thus the per cell per day probability for a given cell in the primary mass to disseminate and form a metastatic colony at a distant site. To rely to the data and estimate μ^i in a patient i , we assumed that the LDH level was a surrogate of the total metastatic mass, whereas the SIOPEN score reflected the visible metastases only (see Figure 1 and Methods). We also used the primary tumor size at diagnosis to infer the age of the tumor and simulate the pre-diagnosis history of the disease. This analysis resulted in predicted ages of 75 ± 4 days (mean \pm standard deviation, media 76 days) between the first cancer cell and diagnosis. The model was able to accurately reproduce the LDH levels (Figure 3A). Descriptive power of the SIOPEN score was much less important (Figure 3B), with most patients either predicted to have no visible metastatic mass (SIOPEN = 0) despite visible metastases in the data (SIOPEN >0), or conversely. The parameter $\ln \mu$ revealed no correlation with either the log(LDH) (R = 0.25) or the SIOPEN (R = 0.201, Figure 3C), suggesting independent added value of this parameter – possibly informative of progression or survival – as compared to the data alone.

B. Validation of the model

We proved previously our mechanistic modeling of tumoral growth and expansion was valid, since it is able in one hand to estimate the tumoral evolution (Figure 1) and in another hand to reproduce other parameters as LDH rate or SIOPEN scores, without limiting himself to them. Indeed, the model fit with one only patient-specific parameter: the μ value, which is an independent factor from LDH rate, SIOPEN score, or any clinical variable. (Figure 3).

C. Survival analyses and Prognosis Value of the Model (Figure 6)

PFS Analyses: μ value was not statistically significantly associated with PFS (p=0.475) in KM analyses. But a tendency seems to appear using a Cox regression model including all individual features for μ value (HR of 0.754 (IC 0.559-1.02), p=0.0639). On the other hand, multivariate Cox

regression model with all features or only significant features shows again a statistically significant association between LDH rate and PFS (respectively HR=2.48 (IC=0.995-6.16), p=0.0513 and HR=1.75 (IC 1.04-2.96), p=0.0363). MCI of the model is 0.52 for PFS.

OS Analyses: In KM analyses, μ value seems to be associated with OS (p=0.105). With a statistically significant difference in Cox regression model including all individual features for μ with an HR of 0.667 (IC 0.484-0.919), p=0.0133), confirmed in Cox regression model including only significant features with HR=0.655 (IC 0.468-0.916), p=0.0134. On the other hand, multivariate Cox regression model with all features or only significant features shows again a statistically significant association between LDH rate and OS (Respectively HR=4.2 (IC=1.6-11), p=0.00349 and HR=4.49 (IC 1.82-11.1), p=0.00111). MCI of the model is 0.66 for OS.

VI. Determination of an Ultra High-Risk Neuroblastoma?

No parameter seems to be statistically significantly associated with precocious relapse (>18months) even according to our model. (Figure 7)

VII. Discussion

We report here about the development of a mathematical modeling of metastatic neuroblastoma using a semi-mechanistic model. The model is based on usual risk factors, easy to collect at diagnosis and used routinely by clinicians, for a better relevance, from a cohort of 49 patients with HRNB, all treated according to HR-NBL1 recommendations. Our model can adequately describe metastatic spreading but also to significantly predict outcomes for patients. We introduce a new clinic-biologico-mathematical factor, μ , that is a reflect of the capacity of the tumor to generate metastases.

Tumor growth is a complex biological process, that includes tumoral proliferation regulation abnormalities of cancer stem cells (38), neoangiogenesis (32,33), microenvironnement interactions (38,39) immune interactions between tumoral cells and immune regulation mechanisms (4),(39–41). These complex interacting processes are regulated by many genes or epigenetic regulators (42) currently still being identified. How to model these complex properties remains an open debate. We have used a mechanistic approach relying on the metastatic spreading and human clinico-radiological data to model neuroblastoma growth. Such mechanistic models have already been used for different kind of cancers as renal (21) breast (24) or lung cancer (43).

They allow global tumoral volume progression estimation according to time based not only on clinico-biological data but also can incorporate therapeutic effects (i.e. surgery, chemotherapy) or cancer cells interaction to describe and predict tumoral dynamics. Moreover, the limited number of parameters used in these models allows a quick translation to potential clinical applications.

A very limited number of studies have focused on the mathematical modeling of neuroblastoma genesis, growth and metastatic evolution. Indeed, Ciccolini and al. in 2017 (44) have reported a mechanistic model of neuroblastoma, using a classical Gompertzian model. Anyhow, their model was used to optimize gemcitabine metronomic chemotherapy administration but did not intend to model tumor growth. Elsewhere, He and al. in 2018 (45) coupled a complex vasculature model fitting the dynamic growth of the human neuroblastoma cell line IMR32 in mice and a PK/PD model of bevacizumab, an anti-VEGF to predict the most effective regimen for this treatment. *Kasemeier-Kulesa and al.* in 2018 (46) have computed a molecular network model of developmental genes and signaling pathways in a 6 gene inputs logic model, using the discrete Boolean logic, and based on 4 cell states (differentiation, proliferation, angiogenesis, apoptosis). The model was able to predict the stage of the human neuroblastoma SHSY5Y and then the outcome of 77 early stage patients. Recently, *Hidalgo and al.* (47) modeled the whole cell signaling pathways data to link t pathways (molecular mechanisms) involved in cancer physiopathology and patient survival. They identified numerous pathways implicated in the activation or deactivation of several cell functions responsible of poor outcomes in patients with neuroblastoma by for instance promoting of proliferation and apoptosis inhibition (TP53), angiogenesis (FASLG), or metastasis (THBS1, PTPN11 and cAMP AFDN).

All the models proposed above are nevertheless not easily translated in the clinics. Therefore, alternatively, although it is not the mainstay, individual molecular profiling has been studied in neuroblastoma (3,4). Several studies explored genome wide associations to predict outcomes for HRNB patients (48,49) but there are not used yet in usual clinical practice and also questioned the relevance of the identified markers, due to the lack of evidence of a cause-and-effect relationship (50)

The model we developed is able to adequately describe metastatic spreading but also to significantly predict outcomes for patients thanks to a new clinic-biologico-mathematical factor, μ , representing the per cell per day probability for a given cell in the primary mass to disseminate and form a metastatic colony at a distant site. This factor is simple, unique, reproducible, is

supported by physiology and clinical experience, and is generated by the model from LDH rates, SIOOPEN score and primary tumoral size.

In our cohort μ is a better prognostic tool than the validated SIOOPEN score at diagnosis and inversely proportional to the LDH rates to predict OS. Interestingly, a high μ factor value is paradoxically an independent and statistically significant factor of better OS in our cohort. This might be explained by 2 hypotheses. According to the first one, patients with high μ value, might have an aggressive neuroblastoma with a high replicative potential. It may explain a better sensitivity to chemotherapy and therefore better survival for these patients (51). According the second hypothesis, patients with low μ value have a bigger tumoral burden, but are slower progressor (52) or differentiate in more mature form of neuroblastoma. This is consistent with the fact that μ factor is a good prognosis factor for OS but not for PFS. To further confirm one of the two hypotheses, linking μ to molecular analysis of the tumor should be able to unveil the molecular pathways involved and then the behavior of the tumor. The micro-environment and more specifically the immune system might also be implicated in slow tumoral progression and a host's tumoral long-term control. Therefore, correlation between high μ and molecular or immunologic specificities, could be done by performing an analysis of the immune microenvironment at the tumor level.

One of the current challenges is to identify an Ultra High-Risk Neuroblastoma (UHRNB) group. While no consensus exists to define UHRNB (53) (refractory disease (death in the first 6 months after diagnosis, 5 y EFS <15%, non-response or early relapse after first chemotherapy induction), we chose as criteria relapse or progression in the first 18 months after diagnosis. The model was not able to identify these patients. This may be because our definition of Ultra High Risk was inadequate or, because of the very limited number of such patients in our series.

Our study focuses on a monocentric cohort, whose number of patients is limited. In order to test, with greater power, the value of our model, a larger-scale study would be useful.

On the other hand, we have chosen to study the prognostic factors that can be found at the time of diagnosis, in order to be able to provide as soon as possible therapies adapted to the patients most likely to be unresponsive to a conventional high-risk neuroblastoma treatment. But, currently, in the absence of marker to identify them at diagnosis time, patients with poorer outcome are rather determined according to their response to the induction chemotherapy. For UHRNB patients different approaches must be evaluated such as the double hematopoietic stem

cell transplant (54) Further studies, after UHRNB terminology consensus, are needed to shed light to these subjects.

VIII. Conclusion

We developed a mechanistic mathematical model, using human data and a limited number of usual risk factors required in the clinics. The model can reproduce tumoral spreading of high-risk neuroblastoma in our patients and also predict patient prognosis, better than the SIOPEN score at diagnosis. It also led to the creation of a new risk factors, μ parameter, which seems to be associated with better outcomes in OS in our population. These findings must be confirmed in a larger cohort and the physiological substrate underlying this result shall be explored.

IX. References

1. Cancer facts and figures 2015, American Cancer Society, Inc. All - Recherche Google [Internet]. [cité 29 sept 2019]. Disponible sur: <https://www.google.com/search?client=firefox-b-d&q=Cancer+facts+and+figures+2015%2C+American+Cancer+Society%2C+Inc.+All>
2. Ahmed AA, Zhang L, Reddivalla N, Hetherington M. Neuroblastoma in children: Update on clinicopathologic and genetic prognostic factors. *Pediatr Hematol Oncol.* avr 2017;34(3):165-85.
3. Cohn SL, Pearson ADJ, London WB, Monclair T, Ambros PF, Brodeur GM, et al. The International Neuroblastoma Risk Group (INRG) classification system: an INRG Task Force report. *J Clin Oncol Off J Am Soc Clin Oncol.* 10 janv 2009;27(2):289-97.
4. Cheung N-KV, Dyer MA. Neuroblastoma: Developmental Biology, Cancer Genomics, and Immunotherapy. *Nat Rev Cancer.* juin 2013;13(6):397-411.
5. Whittle SB, Smith V, Doherty E, Zhao S, McCarty S, Zage PE. Overview and recent advances in the treatment of neuroblastoma. *Expert Rev Anticancer Ther.* 3 avr 2017;17(4):369-86.
6. Sokol E, Desai AV. The Evolution of Risk Classification for Neuroblastoma. *Children* [Internet]. 11 févr 2019 [cité 29 sept 2019];6(2). Disponible sur: <https://www.ncbi.nlm.nih.gov/pmc/articles/PMC6406722/>
7. London WB, Castleberry RP, Matthay KK, Look AT, Seeger RC, Shimada H, et al. Evidence for an age cutoff greater than 365 days for neuroblastoma risk group stratification in the Children's Oncology Group. *J Clin Oncol Off J Am Soc Clin Oncol.* 20 sept 2005;23(27):6459-65.

8. Schmidt ML, Lal A, Seeger RC, Maris JM, Shimada H, O’Leary M, et al. Favorable prognosis for patients 12 to 18 months of age with stage 4 nonamplified MYCN neuroblastoma: a Children’s Cancer Group Study. *J Clin Oncol Off J Am Soc Clin Oncol*. 20 sept 2005;23(27):6474-80.
9. Valteau-Couanet D, Schleiermacher G, Sarnacki S, Pasqualini C. [High-risk neuroblastoma treatment strategy: The experience of the SIOOPEN group]. *Bull Cancer (Paris)*. oct 2018;105(10):918-24.
10. Morgenstern DA, Pötschger U, Moreno L, Papadakis V, Owens C, Ash S, et al. Risk stratification of high-risk metastatic neuroblastoma: A report from the HR-NBL-1/SIOOPEN study. *Pediatr Blood Cancer*. 2018;65(11):e27363.
11. Matthay KK, Reynolds CP, Seeger RC, Shimada H, Adkins ES, Haas-Kogan D, et al. Long-term results for children with high-risk neuroblastoma treated on a randomized trial of myeloablative therapy followed by 13-cis-retinoic acid: a children’s oncology group study. *J Clin Oncol Off J Am Soc Clin Oncol*. 1 mars 2009;27(7):1007-13.
12. Ladenstein R, Pötschger U, Pearson ADJ, Brock P, Luksch R, Castel V, et al. Busulfan and melphalan versus carboplatin, etoposide, and melphalan as high-dose chemotherapy for high-risk neuroblastoma (HR-NBL1/SIOOPEN): an international, randomised, multi-arm, open-label, phase 3 trial. *Lancet Oncol*. 2017;18(4):500-14.
13. London WB, Bagatell R, Weigel BJ, Fox E, Guo D, Van Ryn C, et al. Historical time to disease progression and progression-free survival in patients with recurrent/refractory neuroblastoma treated in the modern era on Children’s Oncology Group early-phase trials. *Cancer*. 15 déc 2017;123(24):4914-23.
14. Basta NO, Halliday GC, Makin G, Birch J, Feltbower R, Bown N, et al. Factors associated with recurrence and survival length following relapse in patients with neuroblastoma. *Br J Cancer*. 25 oct 2016;115(9):1048-57.
15. Skipper HE, Schabel FM, Wilcox WS. EXPERIMENTAL EVALUATION OF POTENTIAL ANTICANCER AGENTS. XIII. ON THE CRITERIA AND KINETICS ASSOCIATED WITH « CURABILITY » OF EXPERIMENTAL LEUKEMIA. *Cancer Chemother Rep*. févr 1964;35:1-111.
16. Altrock PM, Liu LL, Michor F. The mathematics of cancer: integrating quantitative models. *Nat Rev Cancer*. déc 2015;15(12):730-45.
17. Benzekry S, Pasquier E, Barbolosi D, Lacarelle B, Barlési F, André N, et al. Metronomic reloaded: Theoretical models bringing chemotherapy into the era of precision medicine. *Semin Cancer Biol*. déc 2015;35:53-61.
18. Barbolosi D, Ciccolini J, Lacarelle B, Barlési F, André N. Computational oncology--mathematical modelling of drug regimens for precision medicine. *Nat Rev Clin Oncol*. avr 2016;13(4):242-54.
19. Multiscale Cancer Modeling [Internet]. [cité 3 oct 2019]. Disponible sur: <https://www.ncbi.nlm.nih.gov/pmc/articles/PMC3883359/>

20. Rajkomar A, Dean J, Kohane I. Machine Learning in Medicine. *N Engl J Med*. 4 avr 2019;380(14):1347-58.
21. Computational Modelling of Metastasis Development in Renal Cell Carcinoma [Internet]. [cité 29 sept 2019]. Disponible sur: <https://www.ncbi.nlm.nih.gov/pmc/articles/PMC4658171/>
22. Bilous M, Serdjebi C, Boyer A, Tomasini P, Pouypoudat C, Barbolosi D, et al. Quantitative mathematical modeling of clinical brain metastasis dynamics in non-small cell lung cancer. *Sci Rep* [Internet]. 10 sept 2019 [cité 3 oct 2019];9. Disponible sur: <https://www.ncbi.nlm.nih.gov/pmc/articles/PMC6736889/>
23. Nicolò C, Périer C, Prague M, MacGrogan G, Saut O, Benzekry S. Machine learning versus mechanistic modeling for prediction of metastatic relapse in breast cancer. *bioRxiv*. 10 mai 2019;634428.
24. Benzekry S, Tracz A, Mastri M, Corbelli R, Barbolosi D, Ebos JML. Modeling Spontaneous Metastasis following Surgery: An In Vivo-In Silico Approach. *Cancer Res*. 1 févr 2016;76(3):535-47.
25. Pang QM, Li K, Ma LJ, Sun RP. Clinical research on neuroblastoma based on serum lactate dehydrogenase. *J Biol Regul Homeost Agents*. mars 2015;29(1):131-4.
26. Dorneburg C, Fischer M, Barth TFE, Mueller-Klieser W, Hero B, Gecht J, et al. LDHA in Neuroblastoma Is Associated with Poor Outcome and Its Depletion Decreases Neuroblastoma Growth Independent of Aerobic Glycolysis. *Clin Cancer Res Off J Am Assoc Cancer Res*. 15 2018;24(22):5772-83.
27. Shulkin BL, Shapiro B. Current concepts on the diagnostic use of MIBG in children. *J Nucl Med Off Publ Soc Nucl Med*. avr 1998;39(4):679-88.
28. Matthay KK, Shulkin B, Ladenstein R, Michon J, Giammarile F, Lewington V, et al. Criteria for evaluation of disease extent by 123I-metaiodobenzylguanidine scans in neuroblastoma: a report for the International Neuroblastoma Risk Group (INRG) Task Force. *Br J Cancer*. 27 avr 2010;102(9):1319-26.
29. Ara T, DeClerck YA. Mechanisms of invasion and metastasis in human neuroblastoma. *Cancer Metastasis Rev*. déc 2006;25(4):645-57.
30. Bleeker G, Tytgat GAM, Adam JA, Caron HN, Kremer LCM, Hooft L, et al. 123I-MIBG scintigraphy and 18F-FDG-PET imaging for diagnosing neuroblastoma. *Cochrane Database Syst Rev*. 29 sept 2015;(9):CD009263.
31. Ladenstein R, Lambert B, Pötschger U, Castellani M-R, Lewington V, Bar-Sever Z, et al. Validation of the mIBG skeletal SIOPEN scoring method in two independent high-risk neuroblastoma populations: the SIOPEN/HR-NBL1 and COG-A3973 trials. *Eur J Nucl Med Mol Imaging*. févr 2018;45(2):292-305.
32. Park JR, Bagatell R, Cohn SL, Pearson AD, Villablanca JG, Berthold F, et al. Revisions to the International Neuroblastoma Response Criteria: A Consensus Statement From the

- National Cancer Institute Clinical Trials Planning Meeting. *J Clin Oncol.* 1 août 2017;35(22):2580-7.
33. Iwata K, Kawasaki K, Shigesada N. A dynamical model for the growth and size distribution of multiple metastatic tumors. *J Theor Biol.* 21 mars 2000;203(2):177-86.
 34. Hartung N. Efficient resolution of metastatic tumor growth models by reformulation into integral equations. *Discrete Contin Dyn Syst - B.* 1 janv 2015;20(2):445.
 35. Spratt JS, Meyer JS, Spratt JA. Rates of growth of human solid neoplasms: Part I. *J Surg Oncol.* oct 1995;60(2):137-46.
 36. ExPASy - Cellosaurus [Internet]. [cité 12 oct 2019]. Disponible sur: <https://web.expasy.org/cellosaurus/>
 37. Harrell FE, Lee KL, Mark DB. Multivariable prognostic models: issues in developing models, evaluating assumptions and adequacy, and measuring and reducing errors. *Stat Med.* 28 févr 1996;15(4):361-87.
 38. Gallik KL, Treffy RW, Nacke LM, Ahsan K, Rocha M, Green-Saxena A, et al. Neural crest and cancer: Divergent travelers on similar paths. *Mech Dev.* 2017;148:89-99.
 39. Borriello L, Seeger RC, Asgharzadeh S, DeClerck YA. More than the genes, the tumor microenvironment in neuroblastoma. *Cancer Lett.* 28 sept 2016;380(1):304-14.
 40. Wilkie KP, Hahnfeldt P. Tumor-immune dynamics regulated in the microenvironment inform the transient nature of immune-induced tumor dormancy. *Cancer Res.* 15 juin 2013;73(12):3534-44.
 41. Vanichapol T, Chutipongtanate S, Anurathapan U, Hongeng S. Immune Escape Mechanisms and Future Prospects for Immunotherapy in Neuroblastoma. *BioMed Res Int.* 2018;2018:1812535.
 42. Jubierre L, Jiménez C, Rovira E, Soriano A, Sábado C, Gros L, et al. Targeting of epigenetic regulators in neuroblastoma. *Exp Mol Med.* 27 2018;50(4):51.
 43. Benzekry S, Lamont C, Beheshti A, Tracz A, Ebos JML, Hlatky L, et al. Classical mathematical models for description and prediction of experimental tumor growth. *PLoS Comput Biol.* août 2014;10(8):e1003800.
 44. Ciccolini J, Barbolosi D, Meille C, Lombard A, Serdjebi C, Giacometti S, et al. Pharmacokinetics and Pharmacodynamics-Based Mathematical Modeling Identifies an Optimal Protocol for Metronomic Chemotherapy. *Cancer Res.* 01 2017;77(17):4723-33.
 45. He Y, Kodali A, Wallace DI. Predictive Modeling of Neuroblastoma Growth Dynamics in Xenograft Model After Bevacizumab Anti-VEGF Therapy. *Bull Math Biol.* 2018;80(8):2026-48.
 46. Kasemeier-Kulesa JC, Schnell S, Woolley T, Spengler JA, Morrison JA, McKinney MC, et al. Predicting neuroblastoma using developmental signals and a logic-based model. *Biophys Chem.* 2018;238:30-8.

47. Hidalgo MR, Amadoz A, Çubuk C, Carbonell-Caballero J, Dopazo J. Models of cell signaling uncover molecular mechanisms of high-risk neuroblastoma and predict disease outcome. *Biol Direct.* 22 2018;13(1):16.
48. Zhang L, Lv C, Jin Y, Cheng G, Fu Y, Yuan D, et al. Deep Learning-Based Multi-Omics Data Integration Reveals Two Prognostic Subtypes in High-Risk Neuroblastoma. *Front Genet [Internet].* 2018 [cité 3 oct 2019];9. Disponible sur: <https://www.frontiersin.org/articles/10.3389/fgene.2018.00477/full>
49. Depuydt P, Koster J, Boeva V, Hocking TD, Speleman F, Schleiermacher G, et al. Meta-mining of copy number profiles of high-risk neuroblastoma tumors. *Sci Data.* 30 2018;5:180240.
50. Salazar BM, Balczewski EA, Ung CY, Zhu S. Neuroblastoma, a Paradigm for Big Data Science in Pediatric Oncology. *Int J Mol Sci.* 27 déc 2016;18(1).
51. Skipper HE, Schabel FM, Mellett LB, Montgomery JA, Wilkoff LJ, Lloyd HH, et al. Implications of biochemical, cytokinetic, pharmacologic, and toxicologic relationships in the design of optimal therapeutic schedules. *Cancer Chemother Rep.* déc 1970;54(6):431-50.
52. Norton L, Massagué J. Is cancer a disease of self-seeding? *Nat Med.* août 2006;12(8):875-8.
53. Morgenstern DA, Bagatell R, Cohn SL, Hogarty MD, Maris JM, Moreno L, et al. The challenge of defining « ultra-high-risk » neuroblastoma. *Pediatr Blood Cancer.* avr 2019;66(4):e27556.
54. Park JR, Kreissman SG, London WB, Naranjo A, Cohn SL, Hogarty MD, et al. A phase III randomized clinical trial (RCT) of tandem myeloablative autologous stem cell transplant (ASCT) using peripheral blood stem cell (PBSC) as consolidation therapy for high-risk neuroblastoma (HR-NB): A Children's Oncology Group (COG) study. *J Clin Oncol.* 20 juin 2016;34(18_suppl):LBA3-LBA3.

X. Figures :

Figure 1: Clinical and Preclinical History of neuroblastoma: simulation of growth and dissemination of neuroblastoma by mechanistic mathematical modeling

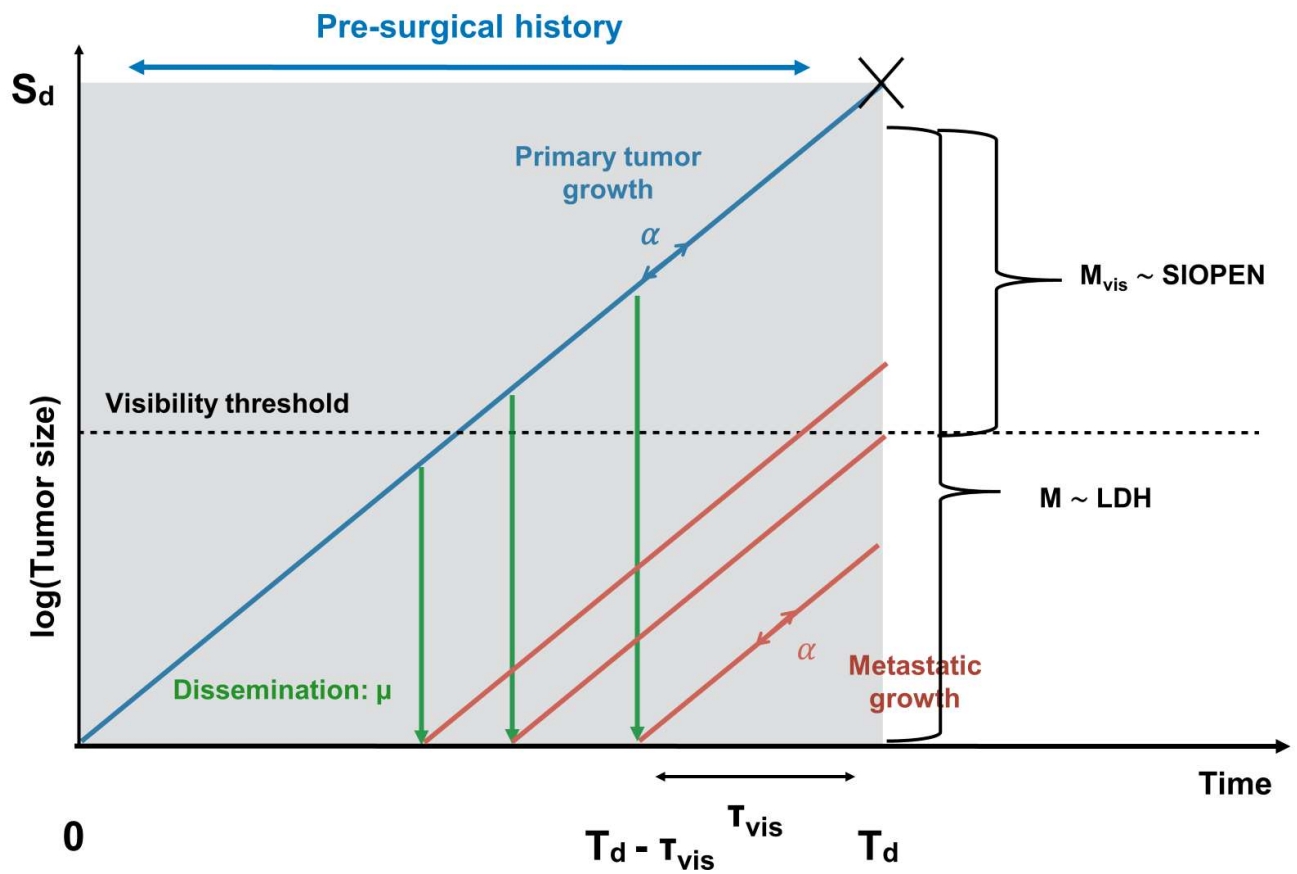


Table 1: Cells line characteristics for establishment of cell doubling time (CDT)

Sex Patients	Female 22,8% (n=13)
	Male 43,9% (n=25)
	Undetermined 33,3% (n=19)
Age Patients	≥ 18 months 45,6% (n=26)
	< 18 months 22,8% (n=13)
	Undetermined 31,6% (n=18)
Stage NRB	II 3,5% (n=2)
	III 7% (n=4)
	IV 31,6% (n=18)
	Undetermined 42,1% (n=33)
NMyc Mutation	Positive 43,9% (n=25)
	Negative 12,3% (n=7)
	Undetermined 43,8% (n=25)

Figure 2: *Patients and Tumor Characteristics*

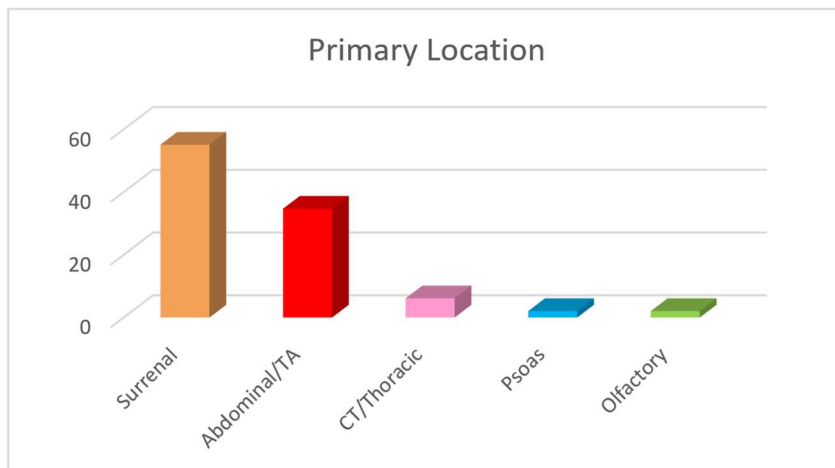
A – General Patients Characteristics

B – Primitive Tumoral Location

C - Metastasis Locations

A	Sex	Male	n= 28 (57,2%)
		Female	n= 21 (42,8%)
	Age	>18 months	n=43 (87,6%)
		<18 months	n=6 (12,2%)
	LDH rates	>1250UI/L	n=18 (36,7%)
		<1250UI/L	n=31 (63,3%)
	MYCN	Amplified	n= 23 (46,9%)
		Non amplified	n=26 (53,1%)
	SIOPEN	>4	n=30 (65,2%)
		<4	n=16 (34,8%)
Métastases	Presence	n= 43 (87,6%)	
	Absence	n= 6 (12,2%)	

B



C

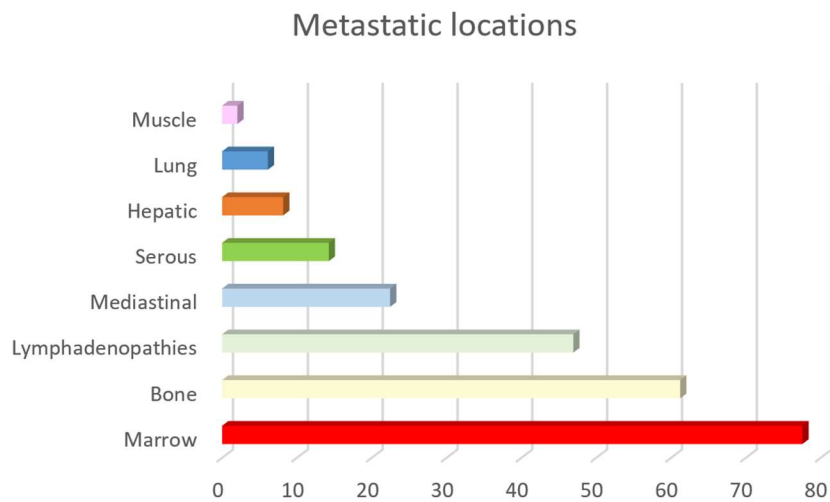


Figure 3: Validation of the model:

A - Fit of the LDH data

B- Fit of the SIOPEN data

C - Correlation matrix of all features including clinical variables and (log) of the mathematical parameter μ . Level of darkness indicates positive correlation whereas brightness indicates negative correlation

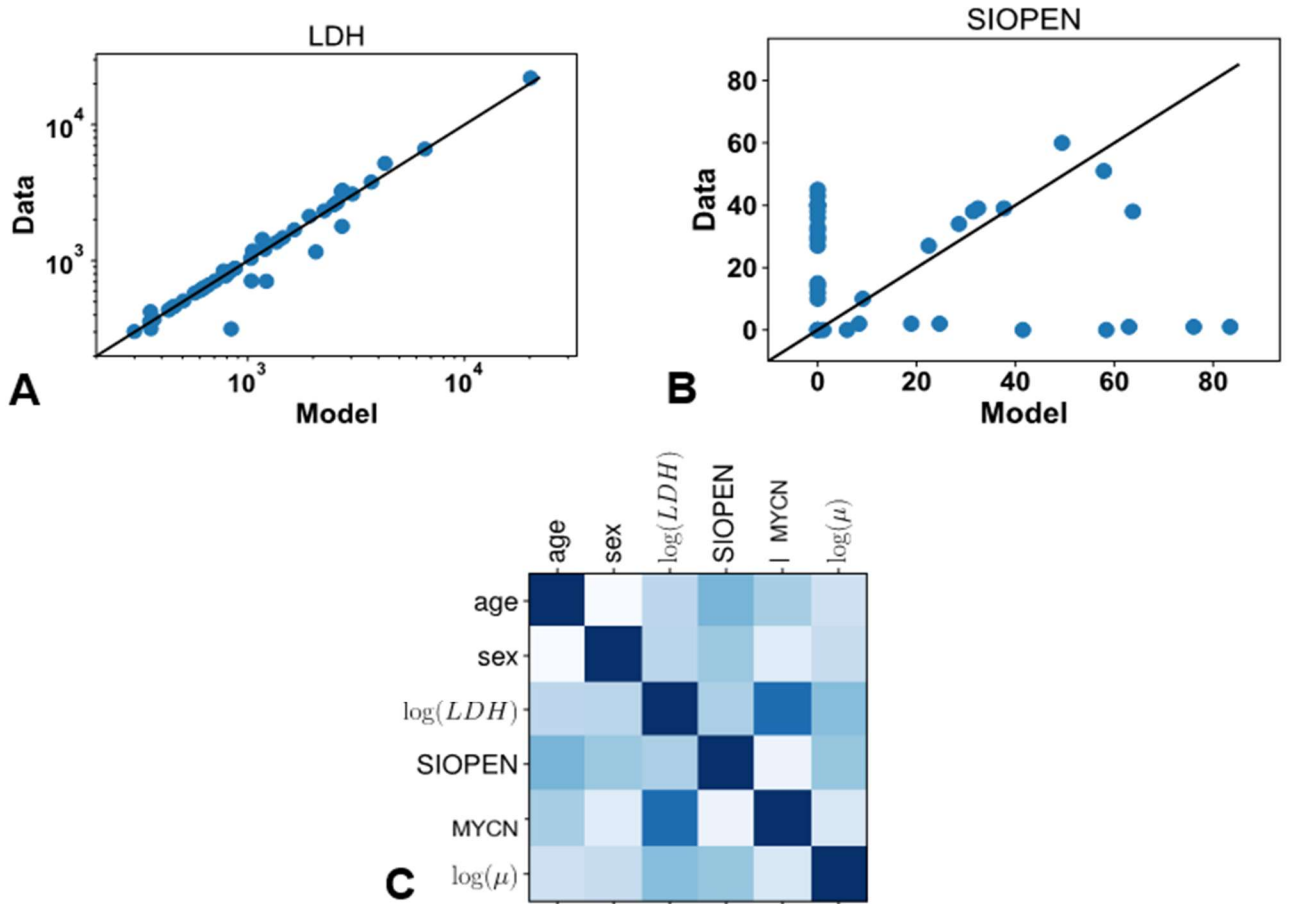


Figure 4: OS and PFS for overall population

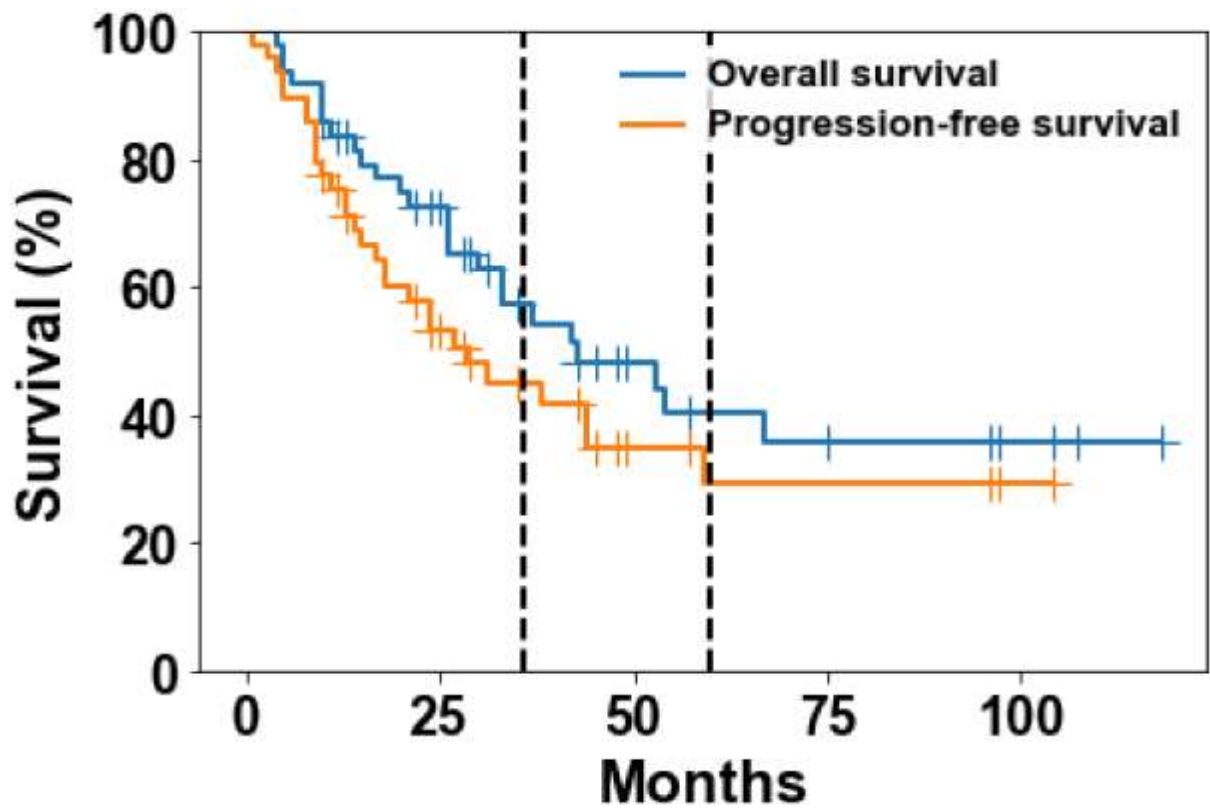


Figure 5: PFS and OS - Classical statistical analysis

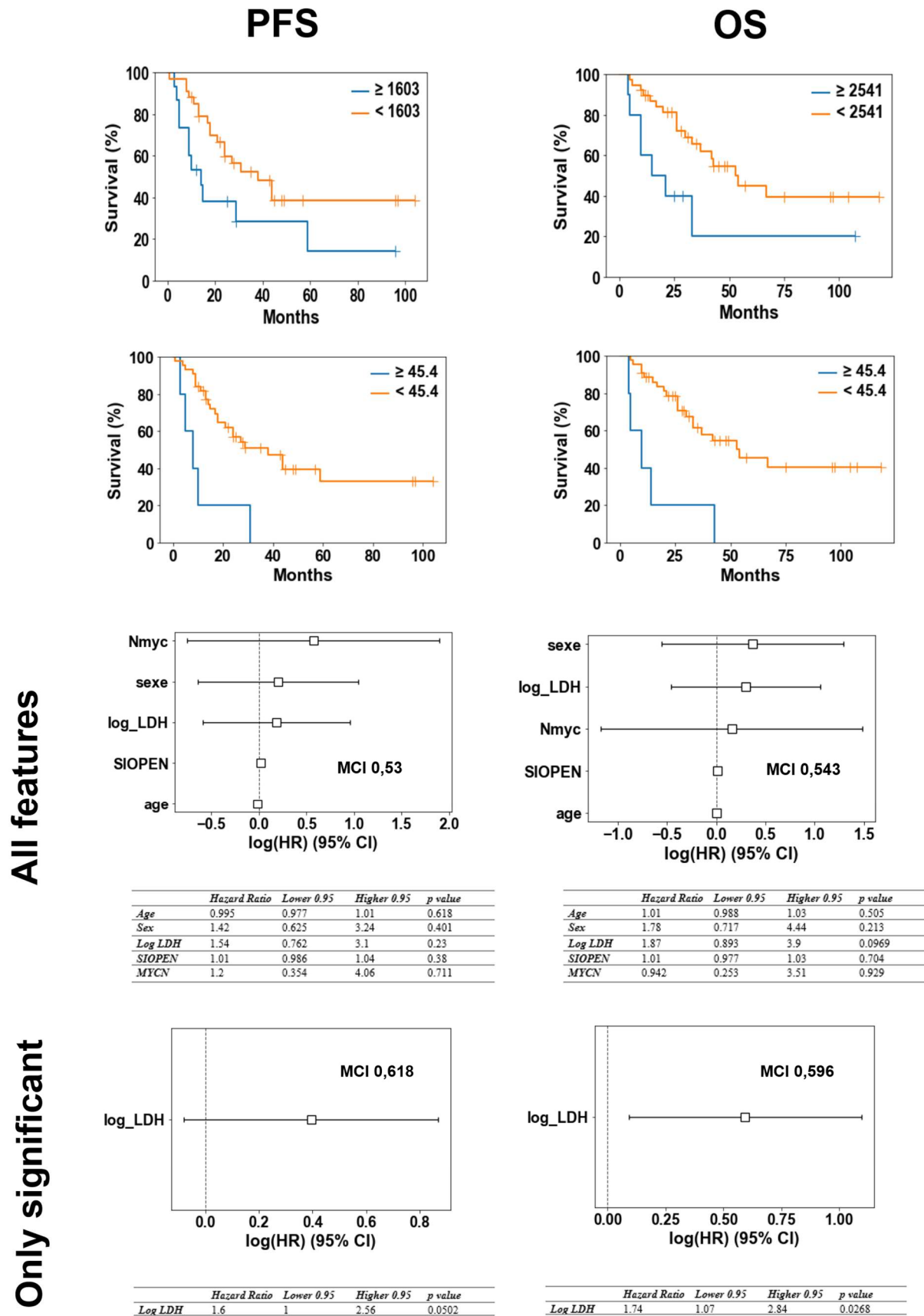


Figure 6: Survival analyses and Prognosis Value of mechanistic model

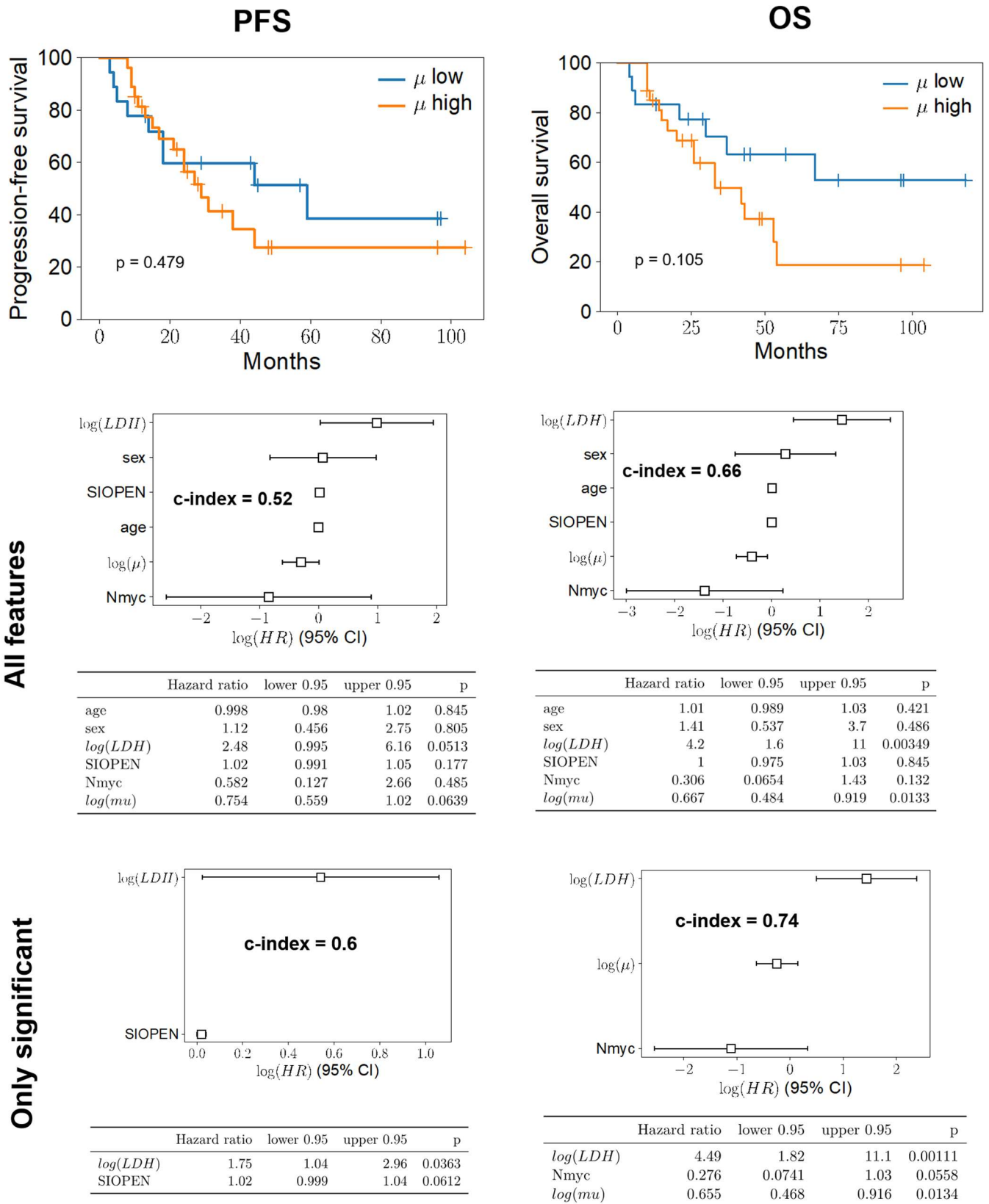


Figure 7: Survival analysis and Research of factors associated with PFS > 18months

A – Univariate

B – Multivariate analysis with only significant variables

C – Multivariate analysis.

A

	HR	Lower 95	Higher 95	p value
Age	1	0.98	1.03	0.722
Sex	0.59	0.17	1.97	0.39
Log LDH	0.48	0.22	0.96	0.0524
SIOPEN	0.99	0.96	1.02	0.615
MYCN	0.37	0.11	1.25	0.117
Log μ	1.1	0.78	1.63	0.602

B

	Odd Ratio	Lower 95	Higher 95	p value
Log LDH	0.52	0.17	1.3	0.197
MYCN	0.83	0.15	4.9	0.836

C

	Odd Ratio	Lower 95	Higher 95	p value
Age	1.01	0.98	1	0.579
Sex	0.67	0.15	2.8	0.586
Log LDH	0.57	0.15	1.8	0.363
SIOPEN	0.99	0.94	1.0	0.553
MYCN	0.62	0.055	6.7	0.689
Log μ	1.13	0.75	1.8	0.571

XI. Appendix

Appendix 1 : Neuroblastoma classification

A. The International Neuroblastoma Staging System (INSS)

B. The INRG Staging System

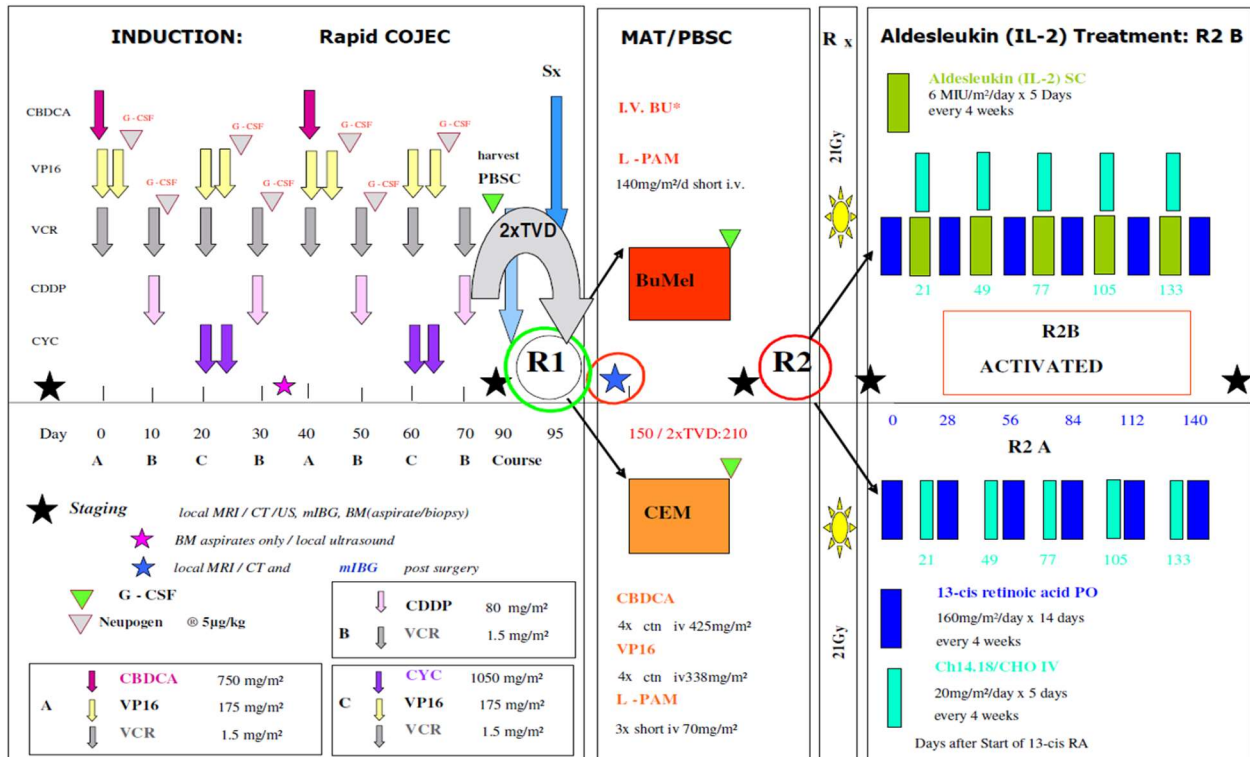
A

Table 4. The International Neuroblastoma Staging System (INSS) [34, 35]	
Stage 1:	Localized tumor* with complete gross excision, with or without microscopic residual disease; representative ipsilateral lymph nodes negative for tumor microscopically (nodes attached to and removed with the primary tumor may be positive).
Stage 2A:	Localized tumor with incomplete gross excision; representative ipsilateral nonadherent lymph nodes negative for tumor microscopically.
Stage 2B:	Localized tumor with or without complete gross excision, with ipsilateral nonadherent lymph nodes positive for tumor. Enlarged contralateral lymph nodes must be negative microscopically.
Stage 3:	Unresectable tumor infiltrating across the midline** with or without regional lymph node involvement; or localized unilateral tumor with contralateral regional lymph node involvement; or midline tumor with bilateral extension by infiltration (unresectable) or by lymph node involvement.
Stage 4:	Any primary tumor with dissemination to distant lymph nodes, bone, bone marrow, liver, skin and/or other organs (except as defined in Stage 4S).
Stage 4S:	Localized primary tumor (as defined for Stage 1, 2A, or 2B), with dissemination limited to skin, liver, and/or bone marrow*** (limited to infants less than one year of age).
* Multifocal primary tumors (e.g., bilateral adrenal primary tumors) should be staged according to the greatest extent of disease, as defined above, and followed by a subscript "M" (e.g., 3 _M).	
** The midline is defined as the vertebral column. Tumors originating on one side and "crossing the midline" must infiltrate to or beyond the opposite side of the vertebral column.	
*** Marrow involvement in stage 4S should be minimal, i.e., less than 10% of total nucleated cells identified as malignant on bone marrow biopsy or on marrow aspirate. More extensive marrow involvement would be considered to be stage 4. The mIBG scan (if done) should be negative in the marrow.	

B

INRG Stage	Age (months)	Histologic Category	Grade of Tumor Differentiation	MYCN	11q Aberration	Ploidy	Pretreatment Risk Group	
L1/L2		GN maturing; GNB intermixed					A Very low	
L1		Any, except GN maturing or GNB intermixed		NA			B Very low	
				Amp			K High	
L2	< 18	Any, except GN maturing or GNB intermixed	Differentiating	NA	No		D Low	
				NA	Yes		G Intermediate	
	≥ 18		GNB nodular; neuroblastoma	Poorly differentiated or undifferentiated	NA	No		E Low
					NA	Yes		H Intermediate
				Amp		N High		
M	< 18			NA		Hyperdiploid	F Low	
	< 12			NA		Diploid	I Intermediate	
	12 to < 18			NA		Diploid	J Intermediate	
	< 18			Amp			O High	
	≥ 18						P High	
MS					No		C Very low	
	< 18			NA	Yes		Q High	
					Amp			R High

Appendix 2 : HRNBL1 Protocol



* Dosage given according to body weight. For details of Busilvex® see Appendix “Drug Information”, 23.9.

R1

ENLARGED ELIGIBILITY CRITERIA ALLOWING **2 TVD** CHEMOTHERAPY CYCLES IN ADDITION, IF INSUFFICIENT RESPONSE TO RAPID COJEC TO REACH PREVIOUS R1 RESPONSE CRITERIA

INFANTS : SPECIAL GUIDELINES AND DRUG DOSING IN THE RELEVANT CHAPTERS OF AMENDED PROTOCOL!

TVD: Topotecan 1.5mg/m²/day for 5 days short infusion, Doxorubicin 22.5mg/m²/24 ctn infusion, Vincristine 1mg/m²/day 48h ctn infusion. SPECIAL GUIDELINES AND DRUG DOSING IN THE RELEVANT CHAPTERS OF AMENDED PROTOCOL!

R2

ENLARGED ELIGIBILITY CRITERIA ALLOWING ALL PATIENTS REGISTERED ON HR-NBL-1/SIOPEN AND HAVING RECEIVED MAT/PBSC TO RECEIVE CH14.18/CHO WITH OR WITHOUT ALDESLEUKIN (IL-2) IF R2 RANDOMISED

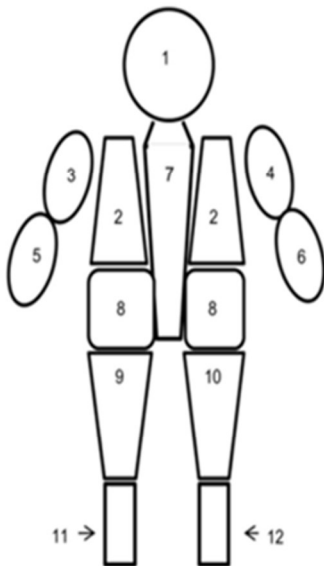
Note:

Once results of R1 become available the superior arm of the randomisation or in case of equivalent results the current standard arm (BUMEL) will be continued until R2 may be closed.

Appendix 3 : Patient Cohort

			primitive						volu							
Age	Sex		mass	Metastases / Local extension	LDH	MYCN	SIOOPEN	MIBG	me	surgery	Response	INRC	DC	OS	Progression	PFS
								neg	(cm3)							
1	45	girl	surrenal	marrow, pulmonary and pleural	1183	0	51	0	1143	0	1	RP	1	14	1	8
2	50	boy	surrenal	nods, marrow, renal and serous	3300	1	45	0	825	1	1	RP	1	15	1	15
3	54	boy	surrenal	bones, marrow and mediastinal	712	1	34	0	434	1	1	RP	1	20	1	13
4	54	girl	surrenal	nods, bones and marrow	1790	1	39	0	273	1	1	RC	0	118	1	59
5	11	boy	surrenal	nods, bones, marrow, mediastinal, renal, pulmonary, medullar canal,	3544	1	0	1		1	1	RP	0	107	1	9
6	50	boy	thoracic	nods, bones, marrow, medullar canal, serous	302	0	33	0	157	0	1	RC	1	42	1	27
7	16	boy	surrenal	nods, bones, marrow, mediastinal, renal, serous	2520	1	0	1	0	0	1	RP	1	5	1	5
8	24	boy	surrenal	bones and marrow	830	0	30	0	10	1	1	RC	0	96	0	96
9	27	boy	dominal	nods, bones, marrow and renal	842	1	2	0	508	1	1	RC	0	104	0	104
10	45	boy	surrenal	nods, bones and marrow	1370	0	27	0	0,5	1	1	RP	0	97	0	97
11	47	boy	surrenal	bones and marrow	508	0	40	0	40	1	1	RC	1	67	1	44
12	13	boy	surrenal	no one	879	1	0	0	189	1	1	RC	1	10	1	9
13	28	boy	cervicothoracic	marrow, medullar canal	882	0	0	0	142	1	1	RC	0	96	0	96
14	21	boy	abdominal	renal	1689	1	1	0	905	1	1	RC	0	96	0	96
15	30	girl	abdominal	nods, bones, renal and serous	2126	1	2	0	258	0	1	RP	1	6	1	4
16	44	girl	surrenal	marrow	1163	0	60	0	385	1	1	RP	1	43	1	31
17	31	boy	surrenal	bones	707	0	38	0	411	1	1	RP	1	54	1	38
18	48	boy	abdominal	nods and marrow	1481	1	0	0	444	1	1	RC	1	53	1	44
19	27	boy	surrenal	bones and marrow	361	0	43	0	41	1	1	RP	0	75	1	8
20	27	girl	surrenal	nods, bones, marrow and hepatic	22022	1	47	0	408	0	0	SD	1	4	1	3
21	140	boy	surrenal	nods, bones and mediastinal	3230	1	53	0	227	1	1	RP	1	10	1	10
22	28	girl	abdominal	nods, marrow, mediastinal and medullar canal	464	0	14	0	75,6	1	1	RP	1	37	1	18
23	36	girl	olfactive	nods, bones and marrow	332	0	18	0	0	0	1	RC	1	26	1	13
24	33	girl	abdominal	nods, marrow and mediastinal	1041	0	40	0	6,9	1	1	RC	0	57	0	57
25	111	boy	surrenal	bones and marrow	317	0	10	0	441	0	1	RP	1	26	1	24
26	33	girl	abdominal	marrow and renal	1216	1	0	0	870	1	1	RP	1	11	1	11
27	74	girl	surrenal	marrow, mediastinal and renal	1437	1	38	0	1099	1	1	RC	0	48	0	48
28	34	girl	abdominal	nods, bones and marrow	712	0	15	0	20,3	1	1	RP	1	30	1	18
29	65	boy	abdominal	nods, bones, marrow, medullar canal and psoas	579	1	0	0	265	0	1	RC	0	49	0	49
30	101	boy	surrenal	nods, bones and marrow	637	1	12	0	61,3	1	1	RC	0	45	0	45
31	25	girl	abdominal	bones, marrow and mediastinal	434	0	29	0	36,4	1	1	RC	0	43	0	43
32	107	boy	surrenal	bones, marrow, medullar canal and hepatic	6628	1	38	0	23,4	1	1	RC	1	21	1	14
33	29	girl	abdominal	bones and marrow	372	0	36	0	132	0	1	RP	1	33	1	24
34	36	boy	surrenal	marrow, renal and pulmonary	2683	1	3	0	105	1	1	RP	1	10	1	9
35	44	boy	abdominal	nods, bones, marrow and mediastinal	316	0	27	0	429	1	1	RC	0	35	0	35
36	26	girl	surrenal	no one	666	0	0	0	187	1	1	RC	0	35	0	35
37	54	boy	surrenal	nods and marrow	2572	1	1	0	46	1	1	RP	1	33	1	29
38	16	girl	abdominal	medullar canal	456	0	0	0	212	1	1	RC	1	26	1	17
39	11	boy	surrenal	nods, marrow and renal	3790	1	0	0	646	1	1	RC	0	29	0	29
40	53	girl	abdominal	bones, marrow and hepatic	773	0	39	0	903	1	1	RC	1	17	1	21
41	22	girl	surrenal	nods and bones	416	0	0	1		1	1	RC	0	31	1	1
42	17	girl	abdominal	bones, marrow, mediastinal, medullar canal, serous and hepatic	356	0	10	0	70,4	1	1	RP	0	28	0	28
43	26	girl	surrenal	nods, bones, renal and serous	3097	1	0	0	926	1	1	RC	0	25	0	25
44	110	boy	thoracique	bones, marrow and medullar canal	618	0	45	0	57	0	1	RP	0	24	0	24
45	47	boy	surrenal	bones and marrow	626	0	32	0	141	1	1	RP	0	22	0	22
46	39	girl	abdominal	nods and marrow	604	0	40	0	84	0	0	SD	0	13	0	13
47	37	boy	surrenal	pancréatique	2328	1	1	0	432	1	1	RP	0	12	0	12
48	21	girl	abdominal	bones, marrow and mediastinal	5198	1	59	0	555	0	1	RP	1	5	1	5
49	38	boy	abdominal	no one	423	0	2	0	410	1	1	RP	0	10	0	10

Appendix 4 : *SIOPEN Scoring*



Before performing sintigraphy, we must avoid interfering treatment and protect thyroid with stable iodine thyroid saturation.

Then, in practice, I123 mIBG is slowly

Injected by periphéric venous pathway

(to avoid side effect), and the radiation gamma

Recording (346keV) come after 24h, with an exposition

Time to radiation <10minutes if patient cooperate.

To score patient, we divide the skeleton in 12 segments, and for each of whom, extension of lesions is noted as :

- 0 : no lesion
- 1 for 1 lesion
- 2 for 2 lesions
- 3 for 3 lesions
- 4 for > 3 lesions but <50% of the concerned segment
- 5 for diffuse disease but <95% of hole segment
- 6 for diffuse disease > 95% of hole segment

Appendix 5 : Cells Doubling Time (36)

<u>Accession/Cell line name</u>	<u>Origin</u>	<u>Sex</u>	<u>Age</u>	<u>Risk Staging</u>	<u>Métastasis</u>	<u>Nmyc</u>	<u>In vivo/vitro</u>	<u>CDT (h)</u>
CVCL9880/VA N BR	H	M	72	STADE II	ABDOMINAL	NC	NC	36
CVCL 6594/CHLA15	H	F	18	NC	MO	NC	NC	21
CVCL 9898/SK N BE(1)	H	M	22	NC	MO	NC	NC	96
CVCL E058/MC NB 1	H	M	24	NC	MO	NC	NC	35
CVCL 7135/SMS MSN	H	M	60	NC	MO	NC	NC	85
CVCLS102/JH	H	M	11	ABDO STADE III	NC	NC	NC	35,7
CVCL B322/KELLY	H	F	12	ALK	NC	NC	NC	35
CVCL AQ17/CHLA 61	H	M	14	NC	NC	NC	NC	102
CVCL 9896/NUB 6	H	NC	21	NC	NC	NC	NC	48
CVLC S099/AS	H	F	33	NC	NC	NC	NC	35,8
CVCL S100/AST	H	M	36	NC	NC	NC	NC	40,7
CVCL IV95/CH9100S	H	F	144	NC	NC	NC	IN VITRO	26
CVCL AQ24/COG N 421	H	M	NC	NC	NC	NC	NC	65
CVLC AQ16/CHLA 53	H	NC	NC	P53	NC	NC	NC	92
CVCL 3041/NB(TU)1	H	F	20	STADE III	NC	NC	NC	49
CVCL IV94/CHP100L	H	F	144	TP53	NC	NC	IN VITRO	21
CVCL 0019/SH SY5Y	H	F	48	IV N TYPE	MO	NEG	NC	50
SKNAS	H				MO	NEG		37
CVCL 2136/NBL 5	H	M	43	NC	NC	NEG	NC	36
SKNAS	H				MO	NEG		37
CVCL 2136/NBL 5	H	M	43	NC	NC	NEG	NC	36
CVCL AQ11/CHLA 12	H	NC	NC	P53	NC	NEG	NC	65
CVCL 0346/IMR 32	H	M	13	METASTATIC	ABDOMINAL	NMYC	IN VITRO	48
CVCL 9896/NUB 7	H	M	6	INTERMEDIATE(1)	ADRENAL	NMYC	NC	38
CVCL 1234/GOTO	H	M	13	NC	ADRENAL	NMYC	NC	48
CVCL 1771/TGW	H	M	23	NC	ADRENAL	NMYC	IN VIVO	32
CVCL 1695/SiMa	H	M	20	NC	ADRENAL	NMYC	NC	74
CVCL 2141/NGP	H	M	30	IV	LUNG	NMYC	NC	60
CVCL 144/NB1	H	M	27	NC	LYMPH NODE	NMYC	NC	45
CVCL 0167/SK N BE(2) M17	H	M	22	IV N TYPE / TP53	MO	NMYC	NC	24
CVCL 2143/NMB	H	F	10	IV NC	MO	NMYC	NC	45
CVCL W474/JK NB1	H	M	12	NC	MO	NMYC	NC	48
CVCL 8904/PER 106	H	M	17	NC	MO	NMYC	IN VITRO	252
CVCL 2548/LA1 55n	H	M	24	NC	MO	NMYC	NC	48
CVCL 7136/SMS SAN	H	F	36	NC	MO	NMYC	NC	71
CVCL 9902/UKF NB 2	H	NC	NC	STADE IV	MO	NMYC	NC	22,5
CVCL 9907/UKF NB 4	H	NC	NC	STADE IV	MO	NMYC	NC	20
CVCL 9904/UKF NB 3	H	NC	NC	STADE IV +	MO	NMYC	NC	22
CVCL 2105/LS	H	F	16	ABDO - STADE III	NC	NMYC	NC	45
CVCL AQ23/COG N 415	H	NC	24	ALK	NC	NMYC	IN VITRO	50
CVCL 5627/NB 1643	H	M	36	ALK - ADRENAL	NC	NMYC	NC	43
CVCL 7133/SMS KCN	H	M	11	ALK - EBV	NC	NMYC	NC	109
CVCL 7131/SMS KAN	H	F	36	N TYPE	NC	NMYC	NC	95
CVCL 1124/CHP134	H	M	13	NC	NC	NMYC	IN VITRO	57,6
CVCL 1123/CHP126	H	F	14	NC	NC	NMYC	IN VITRO	44,5
CVCL AQ25/COG N 440	H	NC	18	NC	NC	NMYC	NC	65
CVCL 1829/LA N 2	H	F	36	STADE II	NC	NMYC	NC	60
CVCL AQ22/COG N 399	H	M	NC	NC	NC	NEG	NC	40
CVCL AQ21/COG N 347	H	M	24	P53	NC	NEG	NC	126
CVCL AQ18/COG N 291	H	NC	NC	P53	NC	NEG	NC	224
IGR N91								66
NB39								48
NB45								240
CHP212								20
HTB10								54
HSNB								50
P.YEUNG 20								50,88
P. YEUNG 50								74,16
P. YEUNG 80								88,56

H: Human, F: Female, M: Male, NEG: Negative, NC: Unknown

Acronyms

Anti GD2 : anti GD2 antibodies (Dinutuximab)

AP-HM : Assistance Publique Hôpitaux de Marseille

CDT : Cell Doubling Time

CTAP scann: Cervico-Thoracic-Abdomino-Pelvic scanner

EFS : Event Free Survival. Event most commonly being progression of the disease, relapse, or death

HR : Hazard Ratio

HRNB : High-Risk Neuroblastoma

IC : Confidence Interval 95%

IL-2: Interleukine 2

INRC : International Neuroblastoma Response Criteria

INGR : International Neuroblastoma Risk Group

KM : Kaplan Meier

LDH : Lactate Deshydrogenase

OS : Overall Survival

MIBG : meta-Iodine-Benzyl-Guanidine

MRI : Magnetic Resonance Imaging

PFS : Progression Free Survival

PCF : Personalized Computerized Folder

PCR : Polymerase Chain Reaction

SIOPEN : International Society of Pediatric Oncology Europe Neuroblastoma Group

UHRNB : Ultra-High-Risk Neuroblastoma

SERMENT D'HIPPOCRATE

Au moment d'être admis(e) à exercer la médecine, je promets et je jure d'être fidèle aux lois de l'honneur et de la probité.

Mon premier souci sera de rétablir, de préserver ou de promouvoir la santé dans tous ses éléments, physiques et mentaux, individuels et sociaux.

Je respecterai toutes les personnes, leur autonomie et leur volonté, sans **aucune discrimination selon leur état ou leurs convictions**. J'interviendrai pour les protéger si elles sont affaiblies, vulnérables ou menacées dans leur intégrité ou leur dignité. Même sous la contrainte, je ne ferai pas **usage de mes connaissances contre les lois de l'humanité**.

J'informerai les patients des décisions envisagées, de leurs raisons et de leurs conséquences.

Je ne tromperai **jamais leur confiance** et **n'exploiterai pas le pouvoir hérité** des circonstances pour forcer les consciences.

Je donnerai mes soins à l'indigent et à quiconque me les demandera. Je ne me laisserai pas influencer par la soif du gain ou la recherche de la gloire.

Admis(e) dans l'intimité des personnes, je tairai les secrets qui me seront confiés. **Reçu(e) à l'intérieur des maisons, je respecterai les secrets des foyers** et ma conduite ne servira pas à corrompre les mœurs.

Je ferai tout pour soulager les souffrances. Je ne prolongerai pas abusivement les agonies. Je ne provoquerai jamais la mort délibérément.

Je préserverai l'indépendance nécessaire à l'accomplissement de ma mission. Je n'entreprendrai rien qui dépasse mes compétences. Je les entretiendrai et les perfectionnerai pour assurer au mieux les services qui me seront demandés.

J'apporterai mon aide à mes confrères ainsi qu'à leurs familles dans l'adversité.

Que les hommes et mes confrères m'accordent leur estime si je suis fidèle à mes promesses ; que je sois déshonoré(e) et méprisé(e) si j'y manque.